

We are IntechOpen, the world's leading publisher of Open Access books Built by scientists, for scientists

4,300

Open access books available

117,000

International authors and editors

130M

Downloads

Our authors are among the

154

Countries delivered to

TOP 1%

most cited scientists

12.2%

Contributors from top 500 universities



WEB OF SCIENCE™

Selection of our books indexed in the Book Citation Index
in Web of Science™ Core Collection (BKCI)

Interested in publishing with us?
Contact book.department@intechopen.com

Numbers displayed above are based on latest data collected.
For more information visit www.intechopen.com



Application of simulated annealing and hybrid methods in the solution of inverse heat and mass transfer problems

Antônio José da Silva Neto¹,
Jader Lugon Junior^{2,5}, Francisco José da Cunha Pires Soeiro¹,
Luiz Biondi Neto¹, Cesar Costapinto Santana³,
Fran Sérgio Lobato⁴ and Valder Steffen Junior⁴

*Universidade do Estado do Rio de Janeiro¹,
Instituto Federal de Educação, Ciência e Tecnologia Fluminense²,
Universidade Estadual de Campinas³,
Universidade Federal de Uberlândia⁴,
Centro de Tecnologia SENAI-RJ Ambiental⁵
Brazil*

1. Introduction

The problem of parameter identification characterizes a typical inverse problem in engineering. It arises from the difficulty in building theoretical models that are able to represent satisfactorily physical phenomena under real operating conditions. Considering the possibility of using more complex models along with the information provided by experimental data, the parameters obtained through an inverse problem approach may then be used to simulate the behavior of the system for different operation conditions. Traditionally, this kind of problem has been treated by using either classical or deterministic optimization techniques (Baltes et al., 1994; Cazzador and Lubenova, 1995; Su and Silva Neto, 2001; Silva Neto and Özişik 1993ab, 1994; Yan et al., 2008; Yang et al., 2009). In the recent years however, the use of non-deterministic techniques or the coupling of these techniques with classical approaches thus forming a hybrid methodology became very popular due to the simplicity and robustness of evolutionary techniques (Wang et al., 2001; Silva Neto and Soeiro, 2002, 2003; Silva Neto and Silva Neto, 2003; Lobato and Steffen Jr., 2007; Lobato et al., 2008, 2009, 2010).

The solution of inverse problems has several relevant applications in engineering and medicine. A lot of attention has been devoted to the estimation of boundary and initial conditions in heat conduction problems (Alifanov, 1974, Beck *et al.*, 1985, Denisov and Solov'yera, 1993, Muniz et al., 1999) as well as thermal properties (Artyukhin, 1982, Carvalho and Silva Neto, 1999, Soeiro et al., 2000; Su and Silva Neto, 2001; Lobato et al., 2009) and heat source intensities (Borukhov and Kolesnikov, 1988, Silva Neto and Özisik, 1993ab, 1994, Orlande and Özisik, 1993, Moura Neto and Silva Neto, 2000, Wang *et al.*, 2000).

in such diffusive processes. On the other hand, despite its relevance in chemical engineering, there is not a sufficient number of published results on inverse mass transfer or heat convection problems. Denisov (2000) has considered the estimation of an isotherm of absorption and Lugon et al. (2009) have investigated the determination of adsorption isotherms with applications in the food and pharmaceutical industry, and Su et al., (2000) have considered the estimation of the spatial dependence of an externally imposed heat flux from temperature measurements taken in a thermally developing turbulent flow inside a circular pipe. Recently, Lobato et al. (2008) have considered the estimation of the parameters of Page's equation and heat loss coefficient by using experimental data from a realistic rotary dryer.

Another class of inverse problems in which the concurrence of specialists from different areas has yielded a large number of new methods and techniques for non-destructive testing in industry, and diagnosis and therapy in medicine, is the one involving radiative transfer in participating media. Most of the work in this area is related to radiative properties or source estimation (Ho and Özisik, 1989, McCormick, 1986, 1992, Silva Neto and Özisik, 1995, Kauati et al., 1999). Two strong motivations for the solution of such inverse problems in recent years have been the biomedical and oceanographic applications (McCormick, 1993, Sundman et al., 1998, Kauati et al., 1999, Carita Montero et al., 1999, 2000).

The increasing interest on inverse problems (IP) is due to the large number of practical applications in scientific and technological areas such as tomography (Kim and Charette, 2007), environmental sciences (Hanan, 2001) and parameter estimation (Souza et al., 2007; Lobato et al., 2008, 2009, 2010), to mention only a few.

In the radiative problems context, the inverse problem consists in the determination of radiative parameters through the use of experimental data for minimizing the residual between experimental and calculated values. The solution of inverse radiative transfer problems has been obtained by using different methodologies, namely deterministic, stochastic and hybrid methods. As examples of techniques developed for dealing with inverse radiative transfer problems, the following methods can be cited: Levenberg-Marquardt method (Silva Neto and Moura Neto, 2005); Simulated Annealing (Silva Neto and Soeiro, 2002; Souza et al., 2007); Genetic Algorithms (Silva Neto and Soeiro, 2002; Souza et al., 2007); Artificial Neural Networks (Soeiro et al., 2004); Simulated Annealing and Levenberg-Marquardt (Silva Neto and Soeiro, 2006); Ant Colony Optimization (Souto et al., 2005); Particle Swarm Optimization (Becceneri et al., 2006); Generalized Extremal Optimization (Souza et al., 2007); Interior Points Method (Silva Neto and Silva Neto, 2003); Particle Collision Algorithm (Knupp et al., 2007); Artificial Neural Networks and Monte Carlo Method (Chalhoub et al., 2007b); Epidemic Genetic Algorithm and the Generalized Extremal Optimization Algorithm (Cuco et al., 2009); Generalized Extremal Optimization and Simulated Annealing Algorithm (Galski et al., 2009); Hybrid Approach with Artificial Neural Networks, Levenberg-Marquardt and Simulated Annealing Methods (Lugon, Silva Neto and Santana, 2009; Lugon and Silva Neto, 2010), Differential Evolution (Lobato et al., 2008; Lobato et al., 2009), Differential Evolution and Simulated Annealing Methods (Lobato et al., 2010).

In this chapter we first describe three problems of heat and mass transfer, followed by the formulation of the inverse problems, the description of the solution of the inverse problems with Simulated Annealing and its hybridization with other methods, and some test case results.

2. Formulation of the Direct Heat and Mass Transfer Problems

2.1 Radiative Transfer

Consider the problem of radiative transfer in an absorbing, emitting, isotropically scattering, plane-parallel, and gray medium of optical thickness τ_0 , between two diffusely reflecting boundary surfaces as illustrated in Fig.1. The mathematical formulation of the direct radiation problem is given by (Özişik, 1973)

$$\mu \frac{\partial I(\tau, \mu)}{\partial \tau} + I(\tau, \mu) = \frac{\omega}{2} \int_{-1}^1 I(\tau, \mu') d\mu', \quad 0 < \tau < \tau_0, \quad -1 \leq \mu \leq 1 \quad (1)$$

$$I(0, \mu) = A_1 + 2\rho_1 \int_0^1 I(0, -\mu') \mu' d\mu', \quad \mu > 0 \quad (2)$$

$$I(\tau_0, \mu) = A_2 + 2\rho_2 \int_0^1 I(\tau_0, \mu') \mu' d\mu', \quad \mu < 0 \quad (3)$$

where $I(\tau, \mu)$ is the dimensionless radiation intensity, τ is the optical variable, μ is the direction cosine of the radiation beam with the positive τ axis, ω is the single scattering albedo, and ρ_1 and ρ_2 are the diffuse reflectivities. The illumination from the outside is supplied by external isotropic sources with intensities A_1 and A_2 .

No internal source was considered in Eq. (1). In radiative heat transfer applications it means that the emission of radiation by the medium due to its temperature is negligible in comparison to the strength of the external isotropic radiation sources incident at the boundaries $\tau = 0$ and/or $\tau = \tau_0$.

In the direct problem defined by Eqs. (1-3) the radiative properties and the boundary conditions are known. Therefore, the values of the radiation intensity can be calculated for every point in the spatial and angular domains. In the inverse problem considered here the radiative properties of the medium are unknown, but we still need to solve problem (1-3) using estimates for the unknowns.

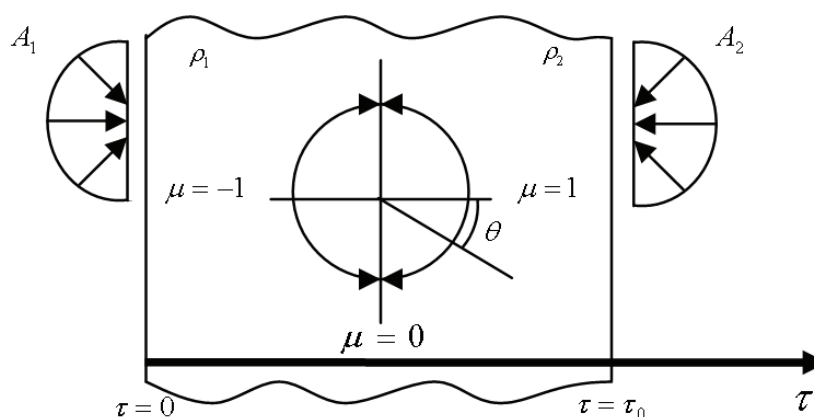


Fig. 1. The geometry and coordinates.

2.2 Drying (Simultaneous Heat and Mass Transfer)

In Fig. 2, adapted from Mwithiga and Olwal (2005), it is represented the drying experiment setup considered in this section. In it was introduced the possibility of using a scale to weight the samples, sensors to measure temperature in the sample, and also inside the drying chamber.

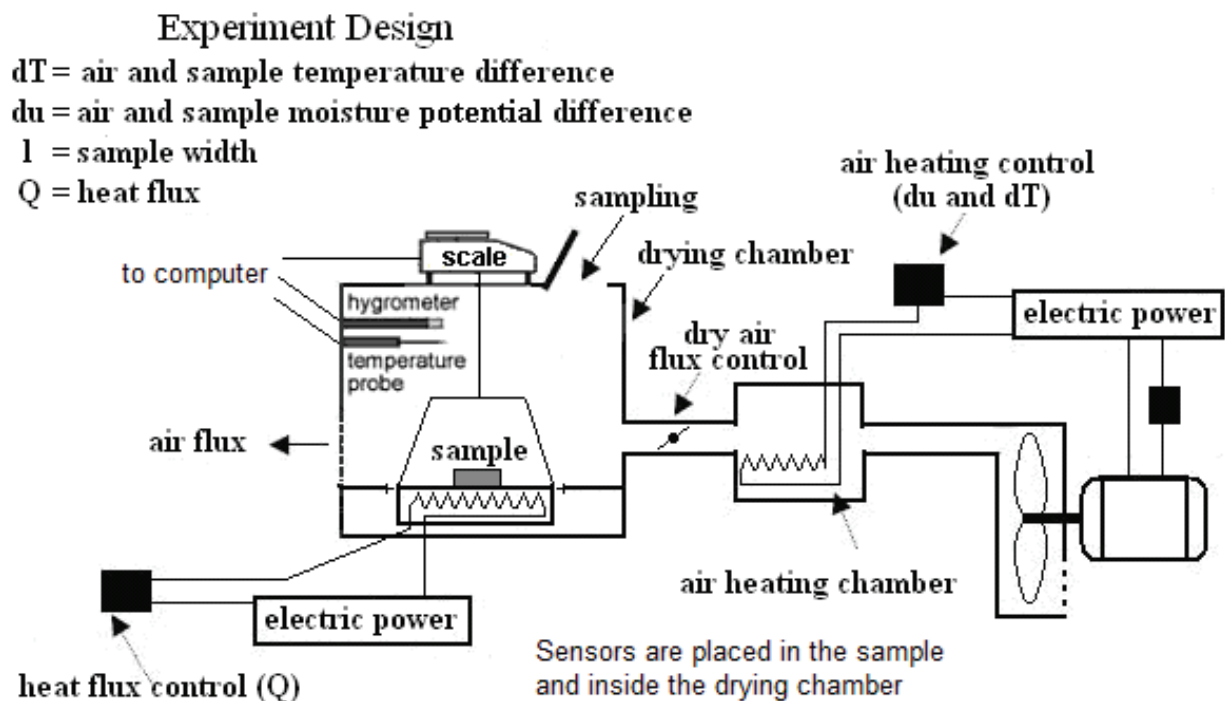


Fig. 2. Drying experiment setup (Adapted from Mwithiga and Olwal, 2005).

In accordance with the schematic representation shown in Fig. 3, consider the problem of simultaneous heat and mass transfer in a one-dimensional porous media in which heat is supplied to the left surface of the porous media, at the same time that dry air flows over the right boundary surface.

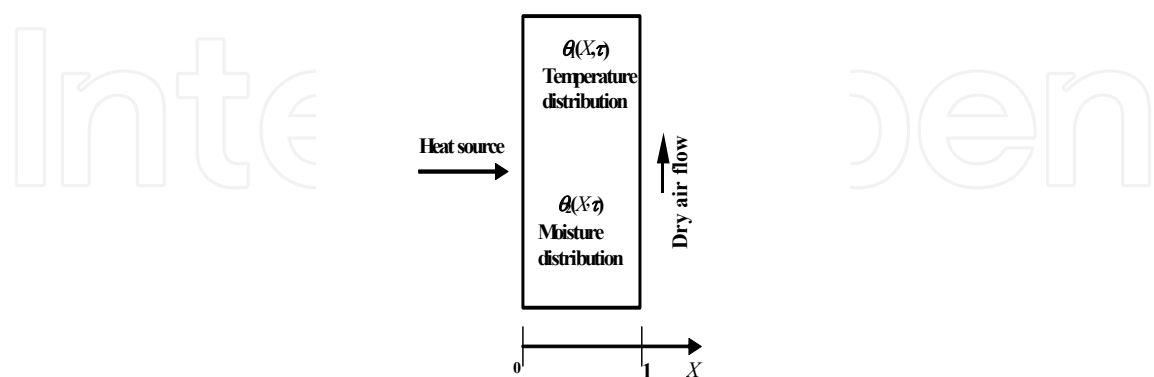


Fig. 3. Drying process schematic representation.

The mathematical formulation used in this work for the direct heat and mass transfer problem considered a constant properties model, and in dimensionless form it is given by (Luikov and Mikhailov, 1965; Mikhailov and Özisik, 1994),

$$\frac{\partial \theta_1(X, \tau)}{\partial \tau} = \alpha \frac{\partial^2 \theta_1}{\partial X^2} - \beta \frac{\partial^2 \theta_2}{\partial X^2}, \quad 0 < X < 1, \quad \tau > 0 \quad (4)$$

$$\frac{\partial \theta_2(X, \tau)}{\partial \tau} = Lu \frac{\partial^2 \theta_2}{\partial X^2} - Lu Pn \frac{\partial^2 \theta_1}{\partial X^2}, \quad 0 < X < 1, \quad \tau > 0 \quad (5)$$

subject to the following initial conditions, for $0 \leq X \leq 1$

$$\theta_1(X, 0) = 0 \quad (6)$$

$$\theta_2(X, 0) = 0 \quad (7)$$

and to the boundary conditions, for $\tau > 0$

$$\frac{\partial \theta_1(0, \tau)}{\partial X} = -Q \quad (8)$$

$$\frac{\partial \theta_2(0, \tau)}{\partial X} = -Pn Q \quad (9)$$

$$\frac{\partial \theta_1(1, \tau)}{\partial X} + Bi_q \theta_1(1, \tau) = Bi_q - (1 - \varepsilon) Ko Lu Bi_m [1 - \theta_2(1, \tau)] = 0 \quad (10)$$

$$\frac{\partial \theta_2(1, \tau)}{\partial X} + Bi_m^* \theta_2(1, \tau) = Bi_m^* - Pn Bi_q [\theta_1(1, \tau) - 1] \quad (11)$$

where

$$\alpha = 1 + \varepsilon Ko Lu Pn \quad (12)$$

$$\beta = \varepsilon Ko Lu \quad (13)$$

$$Bi_m^* = Bi_m [1 - (1 - \varepsilon) Pn Ko Lu] \quad (14)$$

and the dimensionless variables are defined as

$$\theta_1(X, \tau) = \frac{T(x, t) - T_0}{T_s - T_0}, \text{ temperature} \quad (15)$$

$$\theta_2(X, \tau) = \frac{u_0 - u(x, t)}{u_0 - u^*}, \text{ moisture potential} \quad (16)$$

$$X = \frac{x}{l}, \text{ spatial coordinate} \quad (17)$$

$$\tau = \frac{at}{l^2}, \text{ time} \quad (18)$$

$$Lu = \frac{a_m}{a}, \text{ Luikov number} \quad (19)$$

$$Pn = \delta \frac{T_s - T_0}{u_0 - u^*}, \text{ Possnov number} \quad (20)$$

$$Ko = \frac{r}{c} \frac{u_0 - u^*}{T_s - T_0}, \text{ Kossovitch number} \quad (21)$$

$$Bi_q = \frac{hl}{k}, \text{ heat Biot} \quad (22)$$

$$Bi_m = \frac{h_m l}{k_m}, \text{ mass Biot} \quad (23)$$

$$Q = \frac{ql}{k(T_s - T_0)}, \text{ heat flux} \quad (24)$$

When the geometry, the initial and boundary conditions, and the medium properties are known, the system of equations (4-11) can be solved, yielding the temperature and moisture distribution in the media. The finite difference method was used to solve the system (4-11).

Many previous works have studied the drying inverse problem using measurements of temperature and moisture-transfer potential at specific locations of the medium. But to measure the moisture-transfer potential in a certain position is not an easy task, so in this work it is used the average quantity

$$\bar{u}(t) = \frac{1}{l} \int_{x=0}^{x=l} u(x,t) dx \quad (25)$$

or

$$\bar{\theta}_2(\tau) = \int_{X=0}^{X=1} \theta_2(X, \tau) dX \quad (26)$$

Therefore, in order to obtain the average moisture measurements, $\bar{u}(t)$, one have just to weight the sample at each time (Lugon and Silva Neto, 2010).

2.3 Gas-liquid Adsorption

The mechanism of proteins adsorption at gas-liquid interfaces has been the subject of intensive theoretical and experimental research, because of the potential use of bubble and foam fractionation columns as an economically viable means for surface active compounds recovery from diluted solutions, (Özturk et al., 1987; Deckwer and Schumpe, 1993; Graham and Phillips, 1979; Santana and Carbonell, 1993ab; Santana, 1994; Krishna and van Baten, 2003; Haut and Cartage, 2005; Mouza et al., 2005; Lugon, 2005).

The direct problem related to the gas-liquid interface adsorption of bio-molecules in bubble columns consists essentially in the calculation of the depletion, that is, the reduction of solute concentration with time, when the physico-chemical properties and process parameters are known.

The solute depletion is modeled by

$$\frac{dC_b}{dt} = - \frac{6v_g}{(1 - \varepsilon_g) Hd_b} \Gamma \quad (27)$$

where C_b is the liquid solute concentration (bulk), d_b is the bubble diameter, H is the bubble column height, v_g is the superficial velocity (gas volumetric flow rate divided by the area of the transversal section of the column A), and Γ is the surface excess concentration of the adsorbed solute.

The symbol ε_g represents the gas volumetric fraction, which can be calculated from the dimensionless correlation of Kumar (Öztürk et al., 1987),

$$\varepsilon_g = 0.728U - 0.485U^2 + 0.095U^3 \quad (28)$$

where

$$U = v_g \left[\frac{\rho_l^2}{\gamma(\rho_l - \rho_g)g} \right]^{\frac{1}{4}} \quad (29)$$

ρ_l is the liquid density, γ is the surface tension, g is the gravity acceleration, and ρ_g is the gas density.

The quantities Γ and C are related through adsorption isotherms such as:

(i) Linear isotherm

$$\Gamma = B + KC \quad (30)$$

(ii) Langmuir isotherm

$$\Gamma_1 = \frac{1}{a} \left[\frac{K_1(T)C}{1 + K_1(T)C} \right] \quad (31)$$

(iii) Two-layers isotherm

$$\Gamma_t = \Gamma_1 + \Gamma_2 = \frac{K_1(T) \exp(-\lambda \Gamma_1) C [1 + K_2(T) a C]}{a [1 + K_1 \exp(-\lambda \Gamma_1) C]} \quad (32)$$

where Γ_1 and Γ_2 are the excess superficial concentration in the first and second adsorption layers respectively (see Fig. 4).

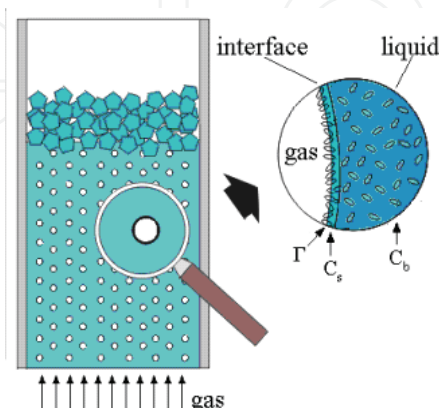


Fig. 4. Schematic representation of the gas-liquid adsorption process in a bubble and foam column.

Considering that the superficial velocity, bubble diameter and column cross section are constant along the column,

$$\frac{\partial \Gamma(z, t)}{\partial z} = \frac{(k_l a) d_b [C_b(t) - C_s(z, t)]}{6v_g} \quad (33)$$

where z represents the spatial coordinate along the column, C_s is the solute concentration next to the bubbles and $(k_l a)$ is the volumetric mass transfer coefficient.

There are several correlations available for the determination of $(k_l a)$ but following the recommendation of Deckwer and Schumpe (1993) we have adopted the correlation of Öztürk et al. (1987) in the solution of the direct problem:

$$Sh = 0,62 Sc^{0,5} Bo^{0,33} Ga^{0,29} \left(\frac{v_g}{\sqrt{g d_b}} \right)^{0,68} \left(\frac{\rho_g}{\rho_l} \right)^{0,04} \quad (34)$$

where

$$Sc = \left(\frac{\nu_l}{D_i} \right), \text{ Schmidt number} \quad (35)$$

$$Sh = \frac{(k_l a) d_b^2}{D_i}, \text{ Sherwood number} \quad (36)$$

$$Bo = \frac{\nu_l}{D_i}, \text{ Bond number} \quad (37)$$

$$Ga = \frac{g d_b^3}{\nu_l^2}, \text{ Galilei Number} \quad (38)$$

D_i is the tensoractive diffusion coefficient and ν_l is the liquid dynamic viscosity.

Combining Eqs. (27) and (33) and using an initial condition, such as $C_b = C_{b0}$ when $t = 0$, and a boundary condition, like $\Gamma = 0$ at $z = 0$, the solute concentration can be calculated as a function of time, $C_b(t)$. Santana and Carbonell (1993ab) developed an analytical solution for the direct problem in the case of a linear adsorption isotherm and the results presented a good agreement with experimental data for BSA (Bovine Serum Albumin).

In order to solve Eq. (27) a second order Runge Kutta method was used, known as the mid point method. Given the physico-chemical and process parameters, as well as the boundary and initial conditions, the solute concentration can be calculated for any time t (Lugon et al., 2009).

3. Formulation of Inverse Heat and Mass Transfer Problems

The inverse problem is implicitly formulated as a finite dimensional optimization problem (Silva Neto and Soeiro, 2003; Silva Neto and Moura Neto, 2005), where one seeks to minimize the cost functional of squared residues between the calculated and experimental values for the observable variable,

$$S(\mathbf{P}) = [\mathbf{G}_{calc}(\mathbf{P}) - \mathbf{G}_{meas}(\mathbf{P})]^T \mathbf{W} [\mathbf{G}_{calc}(\mathbf{P}) - \mathbf{G}_{meas}(\mathbf{P})] = \mathbf{F}^T \mathbf{F} \quad (39a)$$

where \mathbf{G}_{meas} is the vector of measurements, \mathbf{G}_{calc} is the vector of calculated values, \mathbf{P} is the vector of unknowns, \mathbf{W} is the diagonal matrix whose elements are the inverse of the measurement variances, and the vector of residues \mathbf{F} is given by

$$\mathbf{F} = \mathbf{G}_{calc}(\mathbf{P}) - \mathbf{G}_{meas} \quad (39b)$$

The inverse problem solution is the vector $\bar{\mathbf{P}}^*$ which minimizes the norm given by Eq. (39a), that is

$$S(\bar{\mathbf{P}}^*) = \min_{\mathbf{P}} S(\mathbf{P}) \quad (40)$$

Depending on the direct problem, different measurements are to be taken, that is:

a) Radiative problem

Using calculated values given by Eq. (1) and experimental radiation intensities at the boundaries $\tau = 0$ and $\tau = \tau_0$, as well as at points that belong to the set Ω (points inside the domain τ - internal detectors) we try to estimate the vector of unknowns \mathbf{P} considered. Two different vectors of unknowns $\bar{\mathbf{P}}$ are possibly considered for the minimization of the difference between the experimental and calculated values: (i) τ_0, ω, ρ_1 and ρ_2 ; (ii) τ_0, ω, A_1 and A_2 .

b) Drying problem

Using temperature measurements, T , taken by sensors located inside the medium, and the average of the moisture-transfer potential, \bar{u} , during the experiment, we try to estimate the vector of unknowns \mathbf{P} , for which a combination of variables was used: Lu (Luikov number), δ (thermogradients coefficient), r/c (relation between latent heat of evaporation and specific heat of the medium), h/k (relation between heat transfer coefficient and thermal conductivity), and h_m/k_m (relation between mass transfer coefficient and mass conductivity).

c) Gas-liquid adsorption problem

Different vectors of unknowns \mathbf{P} are possibly considered, which are associated with different adsorption isotherms: (i) K and B (Linear isotherm); (ii) $K_1(T)$ and \hat{a} (Langmuir isotherm); (iii) $K_1(T)$, $K_2(T)$, λ and \hat{a} (two-layers isotherm). Here the BSA (Bovine Serum Albumin) adsorption was modeled using a two-layer isotherm.

4. Solution of the Inverse Problems with Simulated Annealing and Hybrid Methods

4.1 Design of Experiments

The sensitivity analysis plays a major role in several aspects related to the formulation and solution of an inverse problem (Dowding et al., 1999; Beck, 1988). Such analysis may be performed with the study of the sensitivity coefficients. Here we use the modified, or scaled, sensitivity coefficients

$$SC_{P_j V(t)} = P_j \frac{\partial V(t)}{\partial P_j}, \quad j = 1, 2, \dots, N_p \quad (41)$$

where V is the observable state variable (which can be measured), P_j is a particular unknown of the problem, and N_p is the total number of unknowns considered.

As a general guideline, the sensitivity of the state variable to the parameter we want to determine must be high enough to allow an estimate within reasonable confidence bounds. Moreover, when two or more parameters are simultaneously estimated, their effects on the state variable must be independent (uncorrelated). Therefore, when represented graphically, the sensitivity coefficients should not have the same shape. If they do it means that two or more different parameters affect the observable variable in the same way, being difficult to distinguish their influences separately, which yields to poor estimations.

Another important tool used in the design of experiments is the study of the matrix

$$\mathbf{SC} = \begin{bmatrix} SC_{P_1 V_1} & SC_{P_2 V_1} & \dots & SC_{P_{N_p} V_1} \\ SC_{P_1 V_2} & SC_{P_2 V_2} & \dots & SC_{P_{N_p} V_2} \\ \dots & \dots & \dots & \dots \\ SC_{P_1 V_m} & SC_{P_2 V_m} & \dots & SC_{P_{N_p} V_m} \end{bmatrix} \quad (42)$$

where V_i is a particular measurement of temperature or moisture potential and m is the total number of measurements.

Maximizing the determinant of the matrix $\mathbf{SC}^T \mathbf{SC}$ results in higher sensitivity and uncorrelation (Beck, 1988).

4.2 Simulated Annealing Method (SA)

Based on statistical mechanics reasoning, applied to a solidification problem, Metropolis et al. (1953) introduced a simple algorithm that can be used to accomplish an efficient simulation of a system of atoms in equilibrium at a given temperature. In each step of the algorithm a small random displacement of an atom is performed and the variation of the energy ΔE is calculated. If $\Delta E < 0$ the displacement is accepted, and the configuration with the displaced atom is used as the starting point for the next step. In the case of $\Delta E > 0$, the new configuration can be accepted according to Boltzmann probability

$$P(\Delta E) = \exp(-\Delta E / k_b T) \quad (43)$$

A uniformly distributed random number p in the interval $[0,1]$ is calculated and compared with $P(\Delta E)$. Metropolis criterion establishes that the new configuration is accepted if $p < P(\Delta E)$, otherwise it is rejected and the previous configuration is used again as a starting point.

Using the objective function $S(\mathbf{P})$, given by Eq. (39a), in place of energy and defining configurations by a set of variables $\{P_i\}, i = 1, 2, \dots, N_p$, where N_p represents the number of unknowns we want to estimate, the Metropolis procedure generates a collection of

configurations of a given optimization problem at some temperature T (Kirkpatrick et al., 1983). This temperature is simply a control parameter. The simulated annealing process consists of first “melting” the system being optimized at a high “temperature”, then lowering the “temperature” until the system “freezes” and no further change occurs. The main control parameters of the algorithm implemented (“cooling procedure”) are the initial “temperature”, T_0 , the cooling rate, r_i , number of steps performed through all elements of vector \mathbf{P} , N_s , number of times the procedure is repeated before the “temperature” is reduced, N_t , and the number of points of minimum (one for each temperature) that are compared and used as stopping criterion if they all agree within a tolerance ε , N_ε .

4.3 Levenberg-Marquardt Method (LM)

The Levenberg-Marquardt is a deterministic local optimizer method based on the gradient (Marquardt, 1963). In order to minimize the functional $S(\mathbf{P})$ we first write

$$\frac{dS}{d\mathbf{P}} = \frac{d}{d\mathbf{P}} (\mathbf{F}^T \mathbf{F}) = 0 \rightarrow \mathbf{J}^T \mathbf{J} = 0 \quad (44)$$

where J is the Jacobian matrix, with the elements $J_{ps} = \partial C_{bp} / \partial P_s$ being $p=1, 2, \dots, M$, and $s=1, 2, \dots, N_p$, where M is the total number of measurements and N_p is the number of unknowns. It is observed that the elements of the Jacobian matrix are related to the scaled sensitivity coefficients presented before.

Using a Taylor’s expansion and keeping only the terms up to the first order,

$$\mathbf{F}(\mathbf{P} + \Delta\mathbf{P}) \cong \mathbf{F}(\mathbf{P}) + \mathbf{J}\Delta\mathbf{P} \quad (45)$$

Introducing the above expansion in Eq. (44) results

$$J^T J \Delta\bar{\mathbf{P}} = -J^T \bar{\mathbf{F}}(\bar{\mathbf{P}}) \quad (46)$$

In the Levenberg-Marquardt method a damping factor γ^n is added to the diagonal of matrix $\mathbf{J}^T \mathbf{J}$ in order to help to achieve convergence.

Equation (46) is written in a more convenient form to be used in the iterative procedure,

$$\Delta\mathbf{P}^n = -[\mathbf{J}^n)^T \mathbf{J}^n + \gamma^n \mathbf{I}]^{-1} (\mathbf{J}^n)^T \mathbf{F}(\mathbf{P}^n) \quad (47)$$

where \mathbf{I} is the identity matrix and n is the iteration index.

The iterative procedure starts with an estimate for the unknown parameters, \mathbf{P}^0 , being new estimates obtained with $\mathbf{P}^{n+1} = \mathbf{P}^n + \Delta\mathbf{P}^n$, while the corrections $\Delta\mathbf{P}^n$ are calculated with Eq. (46). This iterative procedure is continued until a convergence criterion such as

$$|\Delta P_k^n / P_k^n| < \varepsilon, \quad n=1, 2, \dots, N_p \quad (48)$$

is satisfied, where ε is a small number, e.g. 10^{-5} .

The elements of the Jacobian matrix, as well as the right side term of Eq. (47), are calculated at each iteration, using the solution of the problem with the estimates for the unknowns obtained in the previous iteration.

4.4 Artificial Neural Network (ANN)

The multi-layer perceptron (MLP) is a collection of connected processing elements called nodes or neurons, arranged in layers (Haykin, 1999). Signals pass into the input layer nodes, progress forward through the network hidden layers and finally emerge from the output layer (see Fig. 5). Each node i is connected to each node j in its preceding layer through a connection of weight, w_{ij} , and similarly to nodes in the following layer.

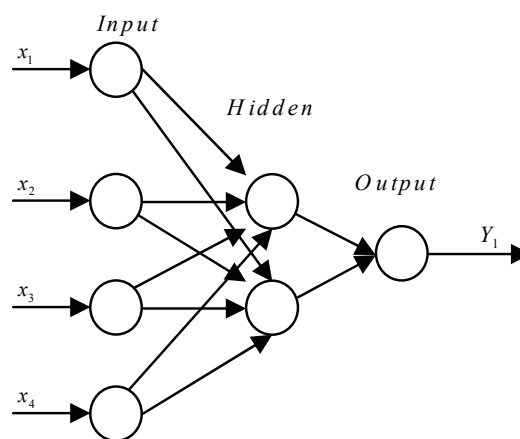


Fig. 5. Multi-layer perceptron network.

A weighted sum is performed at i of all the signals x_j from the preceding layer, yielding the excitation of the node; this is then passed through a nonlinear activation function, f , to emerge as the output of the node x_i to the next layer, as shown by the equation

$$y_i = f\left(\sum_j w_{ij}x_j\right) \quad (49)$$

Various choices for the function f are possible. Here the hyperbolic tangent function $f(x) = \tanh(x)$ is used.

The first stage of using an ANN to model an input-output system is to establish the appropriate values for the connection weights w_{ij} . This is the “training” or learning phase.

Training is accomplished using a set of network inputs for which the desired outputs are known. These are the so called patterns, which are used in the training stage of the ANN. At each training step, a set of inputs are passed forward through the network yielding trial outputs which are then compared to the desired outputs. If the comparison error is considered small enough, the weights are not adjusted. Otherwise the error is passed backwards through the net and a training algorithm uses the error to adjust the connection weights. This is the back-propagation algorithm.

Once the comparison error is reduced to an acceptable level over the whole training set, the training phase ends and the network is established. The parameters of a model (output) may be determined using the real experimental data, which are inputs of the established neural network. This is the generalization stage in the use of the ANN. More details can be found in (Soeiro et al., 2004).

4.5 Differential Evolution

The Differential Evolution (DE) is a structural algorithm proposed by Storn and Price (1995) for optimization problems. This approach is an improved version of the Goldberg's Genetic Algorithm (GA) (Goldberg, 1989) for faster optimization and presented the following advantages: simple structure, easiness of use, speed and robustness (Storn and Price, 1995). Basically, DE generates trial parameter vectors by adding the weighted difference between two population vectors to a third vector. The key parameters of control in DE are the following: N , the population size, CR , the crossover constant and, D , the weight applied to random differential (scaling factor). Storn and Price (1995) have given some simple rules for choosing key parameters of DE for any given application. Normally, N should be about 5 to 10 times the dimension (number of parameters in a vector) of the problem. As for D , it lies in the range 0.4 to 1.0. Initially, $D = 0.5$ can be tried, and then D and/or N is increased if the population converges prematurely.

DE has been successfully applied to various fields such as digital filter design (Storn, 1995), batch fermentation process (Chiou and Wang, 1999), estimation of heat transfer parameters in a bed reactor (Babu and Sastry, 1999), synthesis and optimization of heat integrated distillation system (Babu and Singh, 2000), optimization of an alkylation reaction (Babu and Gaurav, 2000), parameter estimation in fed-batch fermentation process (Wang et al., 2001), optimization of thermal cracker operation (Babu and Angira, 2001), engineering system design (Lobato and Steffen, 2007), economic dispatch optimization (Coelho and Mariani, 2007), identification of experimental data (Maciejewski et al., 2007), apparent thermal diffusivity estimation during the drying of fruits (Mariani et al., 2008), estimation of the parameters of Page's equation and heat loss coefficient by using experimental data from a realistic rotary dryer (Lobato et al., 2008), solution of inverse radiative transfer problems (Lobato et al., 2009, 2010), and other applications (Storn et al., 2005).

4.6 Combination of ANN, LM and SA Optimizers

Due to the complexity of the design space, if convergence is achieved with a gradient based method it may in fact lead to a local minimum. Therefore, global optimization methods are required in order to reach better approximations for the global minimum. The main disadvantage of these methods is that the number of function evaluations is high, becoming sometimes prohibitive from the computational point of view (Soeiro et al., 2004).

In this chapter, different combinations of methods are used for the solution of inverse heat and mass transfer problems, involving in all cases Simulated Annealing as the global optimizer:

- a) when solving radiative inverse problems, it was used a combination of the LM and SA;
- b) when solving adsorption and drying inverse problems, it was used a combination of ANN, LM and SA.

Therefore, in all cases it was run the LM, reaching within a few iterations a point of minimum. After that we run the SA. If the same solution is reached, it is likely that a global

minimum was reached, and the iterative procedure is interrupted. If a different solution is obtained it means that the previous one was a local minimum, otherwise we could run again the LM and SA until the global minimum is reached.

When using the ANN method, after the training stage one is able to quickly obtain an inverse problem solution. This solution may be used as an initial guess for the LM. Trying to keep the best features of each method, we have combined the ANN, LM and SA methods.

5. Test Case Results

5.1 Radiative Transfer

5.1.1 Estimation of $\{\tau_0, \omega, \rho_1, \rho_2\}$ using LM-SA combination

The combined LM-SA approach was applied to several test problems. Since there were no real experimental data available, they were simulated by solving the direct problem and considering the output as experimental data. These results may be corrupted by random multipliers representing a white noise in the measuring equipment. In this effort, since we are developing the approach and trying to compare the performance of the optimization techniques involved, the output was considered as experimental result without any change.

The direct problem is solved with a known vector $\{\tau_0, \omega, \rho_1, \rho_2\}$, which will be considered as the exact solution for the inverse problem. The correspondent output is recorded as experimental data. Now we begin the inverse problem with an initial estimate for the above quantities, obviously away from the exact solution. The described approach is, then, used to find the exact solution.

In a first example the exact solution vector was assumed as $\{1.0, 0.5, 0.95, 0.5\}$ and the initial estimate as $\{0.1, 0.1, 0.1, 0.1\}$. Using both methods the exact solution was obtained. The difference was the computational effort required as shown in Table 1.

| Method | Iterations/Cycles | Number of function evaluations | Final value of the objective function |
|--------|-------------------|--------------------------------|---------------------------------------|
| LM | 8 iterations | 40 | 2.265E-13 |
| SA | 90 cycles | 36000 | 2.828E-13 |

Table 1. Comparison LM – SA for the first example.

In a second example the exact solution was assumed as $\{1.0, 0.5, 0.1, 0.95\}$ and the starting point was $\{5.0, 0.95, 0.95, 0.1\}$. In this case the LM did not converge to the right answer. The results are presented in Table 2.

| Iteration | τ_0 | ω | ρ_1 | ρ_2 | Obj. Function |
|----------------|----------|----------|----------|----------|---------------|
| 0 | 5.0 | 0.95 | 0.95 | 0.1 | 10.0369 |
| 1 | 5.7856 | 9.63E-1 | 6.60E-2 | 1.00E-4 | 1.7664 |
| : | : | : | : | : | : |
| 20 | 9.2521 | 1.0064 | 1.00E-4 | 1.00E-4 | 2.4646 |
| Exact Solution | 1.0 | 0.5 | 0.1 | 0.95 | 0.0 |

Table 2. Results for $Z_{exact} = \{1.0, 0.5, 0.1, 0.95\}$ and $Z_o = \{5.0, 0.95, 0.95, 0.1\}$ using LM.

The difficulty encountered by LM in converging to the right solution was due to a large plateau that exists in the design space for values of τ_0 between 6.0 and 10.0. In this interval the objective function has a very small variation. The SA solved the problem with the same performance as in the first example. The combination of both methods was then applied. SA was let running for only one cycle (400 function evaluations). At this point, the current optimum was {0.94,0.43,0.61,0.87}, far from the plateau mentioned above. With this initial estimate, LM converged to the right solution very quickly in four iterations, as shown in Table 3.

| Iteration | τ_0 | ω | ρ_1 | ρ_2 | Obj. Function [Eq. (39a)] |
|------------|----------|----------|----------|----------|------------------------------|
| 0 | 0.94 | 0.43 | 0.61 | 0.87 | 1.365E-2 |
| 1 | 1.002 | 0.483 | 0.284 | 0.945 | 5.535E-5 |
| : | : | : | : | : | : |
| 4 | 0.999 | 0.500 | 0.100 | 0.9500 | 9.23E-13 |
| Exact Sol. | 1.0 | 0.5 | 0.1 | 0.95 | 0.0 |

Table 3. Results for $Z_{exact} = \{1.0,0.5,0.1,0.95\}$ and $Z_o = \{5.0,0.95,0.95,0.1\}$ using LM after one cycle of SA.

5.1.2 Estimation of $\{\omega, \tau_0, A_1, A_2\}$ using SA and DE

In order to evaluate the performance of the methods of Simulated Annealing and Differential Evolution for the simultaneous estimation of both the single scattering albedo, ω , and the optical thickness, τ_0 , of the medium, and also the intensities A_1 and A_2 of the external sources at $\tau = 0$ and $\tau = \tau_0$, respectively, of a given one-dimensional plane-parallel participating medium, the four test cases listed in Table 4 have been performed (Lobato et al., 2010).

| Parameter | Meaning | Problem | | | |
|-----------|---|---------|-----|-----|-----|
| | | 1 | 2 | 3 | 4 |
| ω | Single scattering albedo | 0.1 | 0.1 | 0.9 | 0.9 |
| τ_0 | Optical thickness of the layer | 0.5 | 5.0 | 0.5 | 5.0 |
| A_1 | Intensity of external source at $\tau = 0$ | 1.0 | 1.0 | 1.0 | 1.0 |
| A_2 | Intensity of external source at $\tau = \tau_0$ | 0.0 | 0.0 | 0.0 | 0.0 |
| n | Number of experimental data points | 20 | 20 | 20 | 20 |

Table 4. Parameters used to define the illustrative examples.

It should be emphasized that 20 points were used for the approximation of the variable μ , and 10 collocation points were taken into account to solve the direct problem. All test cases were solved by using a microcomputer PENTIUM IV with 3.2 GHz and 2 GB of RAM. Both the algorithms were executed 10 times for obtaining the values presented in the Tables (6-9).

The parameters used in the two algorithms are presented in Table 5.

| Parameter | | SA | DE | |
|---|-------------|----------------------|--------------------|--|
| Iteration number | N_{gen} | 100 | 100 | |
| Population size | N | - | 10 | |
| Crossover probability | CR | - | 0.8 | |
| Perturbation rate | D | - | 0.8 | |
| Strategy | - | - | DE/rand/ 1/bin | |
| Temperature number for each temperature | N_{temp} | 50 | - | |
| Temp. initial/final | T_i / T_f | 0.5/0.01 | - | |
| Initial Estimate | Case 1 | [0.25 0.25 0.5 0.5] | Randomly generated | $0 \leq w, \tau_0 \leq 1, 1 \leq A_1 \leq 1.5, 0 \leq A_2 \leq 1$ |
| | Case 2 | [0.25 0.45 0.5 0.5] | | $0 \leq w, A_2 \leq 1, 3 \leq \tau_0 \leq 5, 1 \leq A_1 \leq 1.5$ |
| | Case 3 | [0.75 0.25 0.5 0.5] | | $0 \leq w \leq 1.0 ; 0 \leq \tau_0, A_2 \leq 1 ; 1 \leq A_1 \leq 1.5$ |
| | Case 4 | [0.75 0.45 0.5 0.5] | | $0 \leq w \leq 1.0 ; 3 \leq \tau_0 \leq 5 ; 1 \leq A_1 \leq 1.5 ; 0 \leq A_2 \leq 1$ |

Table 5. Parameters used to define the illustrative examples.

| | | | ω | τ_0 | A_1 | A_2 | Objective Function [Eq. (39a)] |
|-------|----------------------------|---------|---------------|---------------|---------------|---------------|--------------------------------|
| Exact | Error in experimental data | | 0.1 | 0.5 | 1.0 | 0.0 | - |
| DE* | 0.0 | Worst | 0.1003 | 0.5002 | 1.0000 | 0.0001 | 1.5578x10 ⁻⁶ |
| | | Average | 0.0998 | 0.4999 | 0.9999 | 0.0000 | 5.7702x10 ⁻⁷ |
| | | Best | 0.1000 | 0.4999 | 0.9999 | 0.0000 | 4.4564x10⁻⁹ |
| | 0.5% | Worst | 0.1015 | 0.4991 | 0.9980 | 0.0012 | 8.4403x10 ⁻⁴ |
| | | Average | 0.1007 | 0.4985 | 0.9976 | 0.0010 | 8.4244x10 ⁻⁴ |
| | | Best | 0.1006 | 0.4983 | 0.9974 | 0.0011 | 8.4144x10⁻⁴ |
| | 5.0% | Worst | 0.0876 | 0.5018 | 0.9992 | 0.0058 | 0.0842 |
| | | Average | 0.0876 | 0.5018 | 0.9992 | 0.0058 | 0.0842 |
| | | Best | 0.0870 | 0.5017 | 0.9990 | 0.0057 | 0.0842 |
| SA** | 0.0 | Worst | 0.0994 | 0.4999 | 1.0001 | 0.0000 | 5.3920x10 ⁻⁷ |
| | | Average | 0.0996 | 0.4998 | 0.9999 | 0.0000 | 3.4741x10 ⁻⁷ |
| | | Best | 0.0999 | 0.4999 | 0.9999 | 0.0000 | 2.1496x10⁻⁷ |
| | 0.5% | Worst | 0.0944 | 0.4917 | 0.9922 | 0.0001 | 9.6060x10 ⁻⁴ |
| | | Average | 0.0962 | 0.4959 | 0.9970 | 0.0000 | 8.5299x10 ⁻⁴ |
| | | Best | 0.0984 | 0.4976 | 0.9974 | 0.0000 | 8.4058x10⁻⁴ |
| | 5.0% | Worst | 0.0885 | 0.5012 | 0.9991 | 0.0059 | 0.0849 |
| | | Average | 0.0880 | 0.5010 | 0.9990 | 0.0059 | 0.0844 |
| | | Best | 0.0879 | 0.5010 | 0.9989 | 0.0056 | 0.0842 |

* NF=1010, cputime=4.1815 min and ** NF=7015, cputime=30.2145 min.

Table 6. Results obtained for case 1.

| | | | ω | τ_0 | A_1 | A_2 | Objective Function [Eq. (39a)] |
|-------|----------------------------|---------|---------------|---------------|---------------|---------------|-----------------------------------|
| Exact | Error in experimental data | | 0.1 | 5.0 | 1.0 | 0.0 | - |
| DE* | 0.0 | Worst | 0.1024 | 4.9982 | 0.9988 | 0.0013 | 6.3559x10 ⁻⁶ |
| | | Average | 0.1004 | 4.9976 | 0.9992 | 0.0000 | 2.6107x10 ⁻⁶ |
| | | Best | 0.0998 | 5.0036 | 1.0008 | 0.0000 | 1.1856x10⁻⁷ |
| | 0.5% | Worst | 0.0978 | 4.9438 | 0.9844 | 0.0007 | 8.0356x10 ⁻⁴ |
| | | Average | 0.0984 | 4.9470 | 0.9847 | 0.0008 | 8.0333x10 ⁻⁴ |
| | | Best | 0.0983 | 4.9494 | 0.9850 | 0.0010 | 8.0310x10⁻⁴ |
| | 5.0% | Worst | 0.0453 | 4.9678 | 0.9683 | 0.0000 | 0.0878 |
| | | Average | 0.0454 | 4.9675 | 0.9682 | 0.0000 | 0.0878 |
| | | Best | 0.0455 | 4.9674 | 0.9680 | 0.0000 | 0.0878 |
| SA** | 0.0 | Worst | 0.0997 | 5.0097 | 1.0026 | 0.0004 | 8.6468x10 ⁻⁷ |
| | | Average | 0.0998 | 4.9981 | 0.9995 | 0.0003 | 7.7231x10 ⁻⁷ |
| | | Best | 0.0994 | 4.9956 | 0.9988 | 0.0005 | 7.1664x10⁻⁷ |
| | 0.5% | Worst | 0.0929 | 4.9487 | 0.9789 | 0.0009 | 9.4786x10 ⁻³ |
| | | Average | 0.0971 | 4.9256 | 0.9848 | 0.0005 | 8.0999x10 ⁻³ |
| | | Best | 0.0987 | 4.9390 | 0.9841 | 0.0004 | 8.0645x10⁻⁴ |
| | 5.0% | Worst | 0.0483 | 4.9578 | 0.9689 | 0.0001 | 0.0892 |
| | | Average | 0.0484 | 4.9575 | 0.9685 | 0.0001 | 0.0890 |
| | | Best | 0.0485 | 4.9554 | 0.9680 | 0.0001 | 0.0888 |

* NF=1010, cputime=21.4578 min and ** NF=8478, cputime=62.1478 min.
Table 7. Results obtained for case 2.

| | | | ω | τ_0 | A_1 | A_2 | Objective Function [Eq. (39a)] |
|-------|----------------------------|---------|---------------|---------------|---------------|---------------|-----------------------------------|
| Exact | Error in experimental data | | 0.9 | 0.5 | 1.0 | 0.0 | - |
| DE* | 0.0 | Worst | 0.8998 | 0.5001 | 1.0000 | 0.0000 | 4.0332x10 ⁻⁹ |
| | | Average | 0.8999 | 0.5000 | 1.0000 | 0.0000 | 2.1772x10 ⁻⁹ |
| | | Best | 0.9000 | 0.5000 | 1.0000 | 0.0000 | 2.0152x10⁻⁹ |
| | 0.5% | Worst | 0.9028 | 0.4978 | 0.9979 | 0.0001 | 8.9999x10 ⁻³ |
| | | Average | 0.9020 | 0.4980 | 0.9984 | 0.0000 | 8.8788x10 ⁻⁴ |
| | | Best | 0.9018 | 0.4988 | 0.9994 | 0.0000 | 8.6296x10⁻⁴ |
| | 5.0% | Worst | 0.9020 | 0.4700 | 0.9864 | 0.0000 | 0.0776 |
| | | Average | 0.9022 | 0.4790 | 0.9870 | 0.0000 | 0.0746 |
| | | Best | 0.9032 | 0.4807 | 0.9871 | 0.0000 | 0.0736 |
| SA** | 0.0 | Worst | 0.8998 | 0.5000 | 1.0000 | 0.0001 | 8.3002x10 ⁻⁸ |
| | | Average | 0.8998 | 0.5000 | 1.0000 | 0.0000 | 4.7782x10 ⁻⁸ |
| | | Best | 0.8999 | 0.5000 | 1.0000 | 0.0000 | 2.0152x10⁻⁸ |
| | 0.5% | Worst | 0.9039 | 0.4981 | 0.9981 | 0.0000 | 8.7988x10 ⁻⁴ |
| | | Average | 0.9025 | 0.4980 | 0.9986 | 0.0000 | 8.7744x10 ⁻⁴ |
| | | Best | 0.9021 | 0.4990 | 0.9994 | 0.0000 | 8.7014x10⁻⁴ |
| | 5.0% | Worst | 0.9049 | 0.4790 | 0.9859 | 0.0000 | 0.0760 |
| | | Average | 0.9024 | 0.4792 | 0.9860 | 0.0000 | 0.0756 |
| | | Best | 0.9030 | 0.4800 | 0.9864 | 0.0000 | 0.0738 |

* NF=1010, cputime=3.8788 min and ** NF=8758, cputime=27.9884 min.
Table 8. Results obtained for case 3.

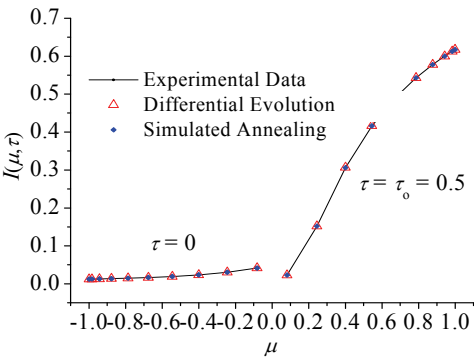
| | | | ω | τ_0 | A_1 | A_2 | Objective Function [Eq.(39)] |
|-------|----------------------------|---------|---------------|---------------|---------------|---------------|---------------------------------|
| Exact | Error in experimental data | | 0.9 | 5.0 | 1.0 | 0.0 | - |
| DE* | 0.0 | Worst | 0.9000 | 5.0002 | 0.9996 | 0.0000 | 2.8555x10 ⁻⁸ |
| | | Average | 0.9000 | 5.0001 | 0.9999 | 0.0000 | 2.6683x10 ⁻⁸ |
| | | Best | 0.9000 | 5.0000 | 0.9999 | 0.0000 | 2.6203x10⁻⁸ |
| | 0.5% | Worst | 0.8985 | 5.0043 | 1.0040 | 0.0008 | 7.8547x10 ⁻⁴ |
| | | Average | 0.8990 | 5.0030 | 1.0038 | 0.0009 | 7.5553x10 ⁻⁴ |
| | | Best | 0.8993 | 5.0023 | 1.0028 | 0.0009 | 7.4263x10⁻⁴ |
| | 5.0% | Worst | 0.8999 | 5.0599 | 1.0118 | 0.0001 | 0.0844 |
| | | Average | 0.8992 | 5.0592 | 1.0117 | 0.0000 | 0.0824 |
| | | Best | 0.8979 | 5.0562 | 1.0107 | 0.0000 | 0.0804 |
| SA** | 0.0 | Worst | 0.9001 | 5.0003 | 0.9998 | 0.0000 | 3.7788x10 ⁻⁸ |
| | | Average | 0.9000 | 5.0002 | 0.9999 | 0.0000 | 2.9988.x10 ⁻⁸ |
| | | Best | 0.9000 | 5.0000 | 0.9999 | 0.0000 | 2.7245x10⁻⁸ |
| | 0.5% | Worst | 0.8988 | 5.0034 | 1.0040 | 0.0009 | 7.9877x10 ⁻⁴ |
| | | Average | 0.8989 | 5.0033 | 1.0040 | 0.0009 | 7.7747x10 ⁻⁴ |
| | | Best | 0.8990 | 5.0033 | 1.0041 | 0.0009 | 7.5245x10⁻⁴ |
| | 5.0% | Worst | 0.8999 | 5.0692 | 1.0090 | 0.0001 | 0.0855 |
| | | Average | 0.8994 | 5.0691 | 1.0189 | 0.0001 | 0.0834 |
| | | Best | 0.8981 | 5.0566 | 1.0179 | 0.0001 | 0.0811 |

* NF=1010, *cputime*= 16.3987 min and ** NF=8588, *cputime*= 58.9858 min.

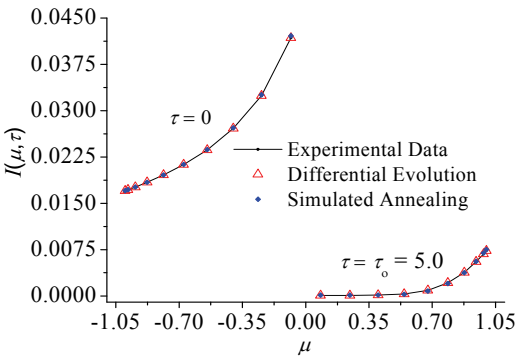
Table 9. Results obtained for case 4.

The comparisons between the two algorithms are done according to the perspective of both the number of function evaluations (*NF*) and the running time (*cputime*) given in minutes. The present case studies used synthetic experimental data considering 20 control elements to discretize μ and 20 control elements for τ , resulting in 400 synthetic experimental points, that is, 40 (2 x 20) representing points along the boundaries and 360 (18 x 20) inside the domain.

In Table 6 the results obtained for case 1 are presented. It can be observed that when using noiseless data both algorithms presented good estimates for the unknown parameters. However, if noise is increased, it can be observed that the optimal values of the parameters demonstrate that the estimates are poorer. The same behavior was observed for test cases 2-4 whose results are presented in Tables 7-9, respectively. However, the results obtained can be considered satisfactory.



Case 1: $\omega=0.1$, $\tau_0=0.5$, $A_1=1$ and $A_2=0$.



Case 2: $\omega=0.1$, $\tau_0=5.0$, $A_1=1$ and $A_2=0$.

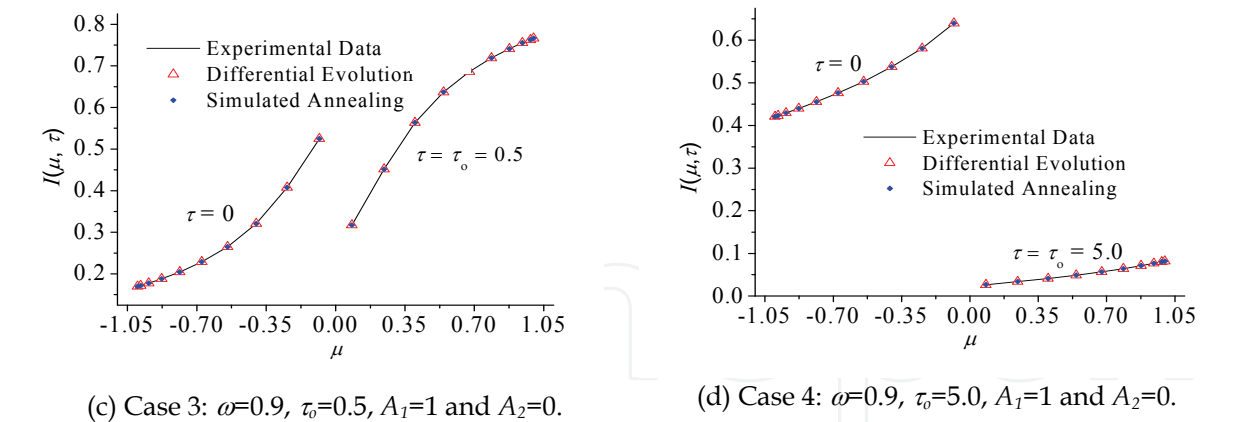


Fig. 6. Radiance generated by using DE and SA - without noise.

Figure 6 illustrates the results presented in Tables 6 to 9 obtained for the radiation intensities using the estimates for the radiative properties, which are now shown on a graphical form for the case without noise in the experimental data.

5.2 Drying (Simultaneous Heat and Mass Transfer)

Much research effort has already been made in order to estimate the Possnov, Kossovitch, heat Biot and mass Biot numbers (Dantas et al., 2003; Huang and Yeh, 2002; Lugon and Silva Neto, 2004), but it was only considered the possibility of optimizing the number and location of temperature sensors, experiment duration, etc. In this work instead, δ , r/c , h/k and h_m/k_m are estimated using an “optimum” experiment (Dowding et al., 1999 and Beck, 1988) for wood drying, and doing so, it was considered also the following process control parameters: heat flux, Q , the medium width, l , the difference between the medium and the air temperatures, $dT = T_s - T_0$, and the difference between the moisture potential between the medium and the air, $du = u_0 - u^*$.

There is no difference between the sensitivity coefficients for the two sets of variable, that is, the scaled sensitivity coefficients are exactly the same for both vectors $\{Lu, Pn, Ko, Bi_q, Bi_m, \varepsilon\}^T$ and $\{Lu, \delta, r/c, h/k, h_m/k_m, \varepsilon\}^T$,

$$SC_{\delta}(X, \tau) = \delta \frac{\partial V(X, \tau)}{\partial \delta} = Pn \frac{\partial V(X, \tau)}{\partial Pn} = SC_{Pn}(X, \tau) \tag{50}$$

$$SC_{r/c}(X, \tau) = r/c \frac{\partial V(X, \tau)}{\partial r/c} = Ko \frac{\partial V(X, \tau)}{\partial Ko} = SC_{Ko}(X, \tau) \tag{51}$$

$$SC_{h/k}(X, \tau) = h/k \frac{\partial V(X, \tau)}{\partial h/k} = Bi_q \frac{\partial V(X, \tau)}{\partial Bi_q} = SC_{Bi_q}(X, \tau) \tag{52}$$

$$SC_{h_m/k_m}(X, \tau) = h_m/k_m \frac{\partial V(X, \tau)}{\partial h_m/k_m} = Bi_m \frac{\partial V(X, \tau)}{\partial Bi_m} = SC_{Bi_m}(X, \tau) \tag{53}$$

The reasons for changing the estimated variables are the use of the design of experiment tools and interpretation. Consider the heat and mass Biot numbers for example. If one changes the media width, l , both heat and mass Biot numbers changes. The mathematical

problem would be different, even though the material is still the same, because one is estimating two different heat and mass Biot numbers. In order to solve this problem, it was decided to estimate the relation between heat transfer coefficient and thermal conductivity, h/k , and the relation between mass transfer coefficient and mass conductivity, h_m/k_m , so that we could change the media width and continue with the same value for both variables to be estimated.

The same idea was used, choosing to estimate the thermogradient coefficient (δ) and the relation between latent heat of evaporation and specific heat of the medium (r/c), instead of the Possnov (Pn) and Kossovitch (Ko) numbers. Doing so, one is able to optimize the experiment considering the difference between the medium and the air temperatures, $dT = T_s - T_0$, and the difference between the moisture-transfer potential between the media and the air, $du = u_0 - u^*$, without affecting the estimated parameters values.

In Fig. 7 it is represented the variation of the value of the matrix $\mathbf{SC}^T\mathbf{SC}$ determinant as a function of the temperature differences and moisture potential differences between the medium and the air flowing over it. It is not difficult to understand that one could not build such a graph using a vector of unknown parameters containing Possnov (Pn) and Kossovitch (Ko) numbers. In order to achieve greater sensitivities, while the temperature difference has to be the lowest, the moisture potential difference has to be the highest possible. The solid square represents the chosen designed experiment, considering the existence of practical difficulties that may limit our freedom of choice.

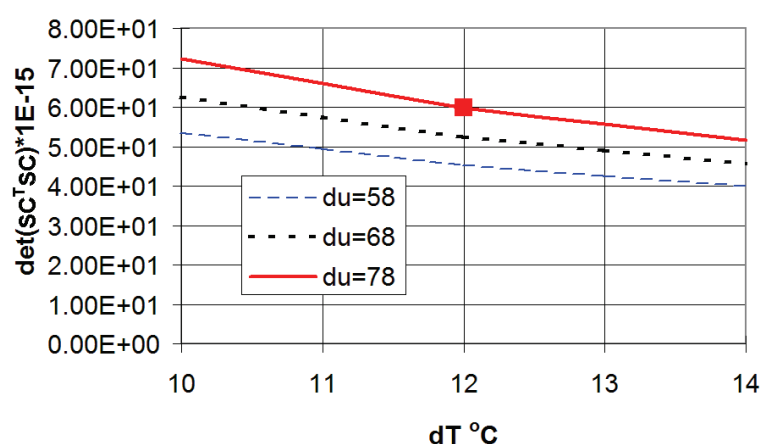


Fig. 7. Determinant of matrix $\mathbf{Y}^T\mathbf{Y}$ as a function of temperature (dT) and moisture potential (du) differences.

In Fig. 8 it is represented the values of the determinant of matrix $\mathbf{SC}^T\mathbf{SC}$ for different values of the heat flux Q and media thickness l . It is also easy to understand that one could not build such a graph using a vector of unknown parameters containing heat and mass Biot numbers. For practical reasons it was chosen to limit the sample temperature to 130° C. In Fig. 8 the same curve has a continuous-line part and a dashed-line one, when the sample temperature exceeds the limit of 130° C. The solid square shows the chosen designed experiment.

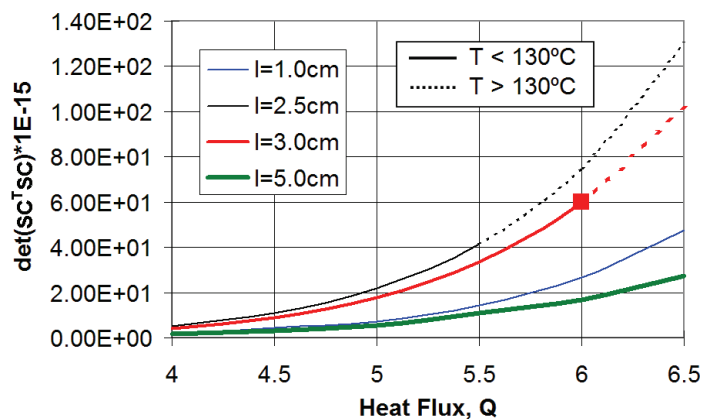


Fig. 8. Determinant of $\mathbf{SC}^T\mathbf{SC}$ matrix for different values of the heat flux Q and medium thickness l .

Considering the previous analysis of the sensitivity graphs and matrix $\mathbf{SC}^T\mathbf{SC}$ determinant, it was designed the experiment whose geometric and process parameters are shown in Table 10. Since the average moisture potential, \bar{u} , is more difficult to measure than temperature, θ_1 , the measurement interval for the average moisture potential, $\Delta\tau_{\bar{u}}$, was considered larger than the interval for the temperature $\Delta\tau_{\theta_1}$.

| Geometric or process parameter | Values | Geometric or process parameter | Values |
|--------------------------------|--------|--------------------------------|--------|
| $dT = T_s - T_0$ | 12 °C | Q | 6.0 |
| T_0 | 24 °C | l | 0.03 m |
| T_s | 36 °C | τ_0 | 0 |
| $du = u_0 - u^*$ | 78 °M | τ_f | 20 |
| u_0 | 86 °M | $\Delta\tau_{\theta_1}$ | 0.2 |
| u^* | 8 °M | $\Delta\tau_{\bar{u}}$ | 1 |
| ε | 0.2 | | |

τ_0 and τ_f represent the initial and sampling times, respectively.
Table 10. Reference values for the designed experiment.

An experiment was designed to perform the simultaneous estimation of Lu , δ , r/c , h/k and h_m/k_m . In order to study the proposed method, since real experiment data were not available, we generated synthetic data using

$$\theta_{lmeas_i} = \theta_{lcalc_i}(\mathbf{P}_{exact}) + \sigma_{\theta_1} r_i, \quad i = 1, 2, \dots, M_{\theta_1} \tag{54a}$$

$$\bar{u}_{meas_i} = \bar{u}_{meas_i}(\mathbf{P}_{exact}) + \sigma_{\bar{u}} r_i, \quad i = 1, 2, \dots, M_{\bar{u}} \tag{54b}$$

where r_i are random numbers in the range $[-1,1]$, M_{θ_1} and $M_{\bar{u}}$ represent the total number of temperature and moisture-transfer potential experimental data, and σ_{θ_1} and $\sigma_{\bar{u}}$ emulates the standard deviation of measurement errors. It was established a standard deviation of

$\sigma_{\theta_1} = 0.03$ considering 100 temperature measurements ($\Delta\tau = 0.2$), resulting in a maximum error of 2%, and $\sigma_{\bar{\theta}_2} = 0.001$ considering 20 moisture measurements ($\Delta\tau = 1.0$), resulting in a maximum error of 4%.

In Fig. 9 the graphics of temperature (θ_1) and moisture potential ($\bar{\theta}_2$) measurements are presented. The continuous line represents the direct problem solution and the squares represent noisy data. In order to show a better representation, only 20 temperature (θ_1) measurements were represented.

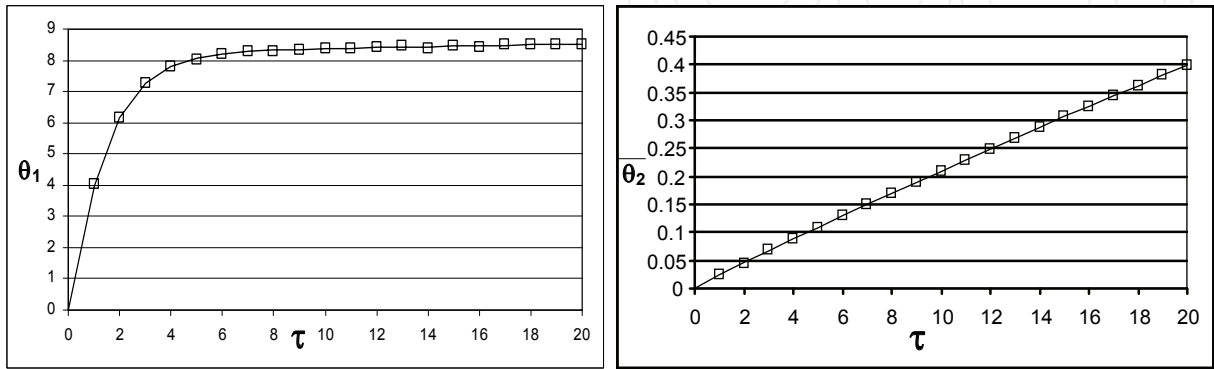


Fig. 9. Temperature (θ_1) and moisture potential ($\bar{\theta}_2$) artificially simulated data.

The results obtained using the methods LM 1 (gradient approximated by FDM – Finite Difference Method), LM 2 (gradient approximated by ANN – Artificial Neural Network), ANN, SA and hybrid combinations, for different levels of noise represented by different values of the standard deviation of measurements errors in temperature and average moisture potential, σ_T and $\sigma_{\bar{u}}$, respectively in Eqs. (54a,b) are shown in Table 11.

| Case | Method | σ_{θ_1} | $\sigma_{\bar{u}}$ | Information | Lu | δ | r/c | h/k | h_m/k_m | Time (s) | S Eq. (39a) |
|------|------------------|---------------------|--------------------|-----------------------------|--------|----------|-------|-------|-----------|----------|---------------|
| - | - | - | - | Exact values | 0.0080 | 2.0 | 10.83 | 34.0 | 114.0 | - | - |
| 1 | LM 1 (grad. FDM) | 0 | 0 | Initial guess | 0.0040 | 1.50 | 8.00 | 20.0 | 80.0 | 15 | 0 |
| | | | | Result $\vec{Z}_{LM^{FDM}}$ | 0.0080 | 2.00 | 10.83 | 34.0 | 114.0 | | |
| 2 | LM 2 (grad. ANN) | 0 | 0 | Initial guess | 0.0040 | 1.50 | 8.00 | 25.0 | 80.0 | 10 | 0 |
| | | | | Result $\vec{Z}_{LM^{ANN}}$ | 0.0080 | 2.00 | 10.83 | 34.0 | 114.0 | | |
| 3 | LM 1 (grad. FDM) | 0.03 | 0.001 | Initial guess | 0.0040 | 1.50 | 8.00 | 20.0 | 80.0 | 15 | 977 |
| | | | | Result $\vec{Z}_{LM^{FDM}}$ | 0.0076 | 2.09 | 10.76 | 34.1 | 121.2 | | |
| 4 | LM 2 (grad. ANN) | 0.03 | 0.001 | Initial guess | 0.0040 | 1.50 | 8.00 | 20.0 | 80.0 | 11 | 897 |
| | | | | Result $\vec{Z}_{LM^{ANN}}$ | 0.0093 | 1.71 | 10.73 | 34.1 | 95.7 | | |

| | | | | | | | | | | | |
|---|--|------|-------|----------------------------------|--------|------|-------|------|-------|-----|------|
| 5 | ANN (without initial guess) | 0.03 | 0.001 | Result \vec{Z}_{ANN} | 0.0083 | 2.10 | 10.04 | 35.0 | 117.1 | 1 | 3190 |
| 6 | LM 1 (grad. FDM) | 0.03 | 0.001 | Initial guess \vec{Z}_{ANN} | 0.0083 | 2.10 | 10.04 | 35.0 | 117.1 | 16 | 974 |
| | | | | Result $\vec{Z}_{LM^{FDM}}$ | 0.0083 | 1.92 | 10.75 | 34.1 | 110.0 | | |
| 7 | LM 2 (grad. ANN) | 0.03 | 0.001 | Initial guess \vec{Z}_{ANN} | 0.0083 | 2.10 | 10.04 | 35.0 | 117.1 | 11 | 903 |
| | | | | Result $\vec{Z}_{LM^{ANN}}$ | 0.0082 | 1.79 | 9.89 | 35.1 | 114.5 | | |
| 8 | SA (SA 20,000 evaluations) | 0.03 | 0.001 | Initial guess | 0.0040 | 1.50 | 8.00 | 25.0 | 80.0 | 300 | 856 |
| | | | | Result \vec{Z}_{SA} | 0.0094 | 1.58 | 9.96 | 35.0 | 98.2 | | |
| 9 | ANN-LM 2-SA (SA 2,000 evaluations) | 0.03 | 0.001 | Initial guess \vec{Z}_{ANN} | 0.0083 | 2.10 | 10.04 | 35.0 | 117.1 | 47 | 760 |
| | | | | Result $\vec{Z}_{LM^{ANN}}$ | 0.0082 | 1.79 | 9.89 | 35.1 | 114.5 | | |
| | | | | Result \vec{Z}_{SA} | 0.0079 | 2.01 | 11.00 | 33.9 | 113.8 | | |
| | | | | Result $\vec{Z}_{LM^{ANN}}$ | 0.0080 | 2.05 | 10.93 | 33.8 | 113.9 | | |

Table 11. Results obtained using LM 1, LM 2, ANN, and hybrid combinations.

One observes that when there is no noise, that is, the standard deviation of measurements errors are zero, the LM method was able to estimate all variables very quickly (see test cases 1 and 2). When noise is introduced, the LM is retained by local minima (test cases 3 and 4); the ANN did not reach a good solution, but quickly got close to it (test case 5). The ANN solution was then used as a first guess for the LM method with good performance in test cases 6 and 7. The SA reached a good solution but required the largest CPU time, and finally the combination of all methods was able to reach a good solution, without being retained by local minima without taking too much time, i.e. one sixth of the SA time. The time shown in the eleventh column of Table 11 corresponds to the CPU time on a Pentium IV 2.8 GHz processor.

5.3 Gas-liquid Adsorption

Recently, the inverse problem of interface adsorption has attracted the attention of an increasing number of researchers (Lugon, 2005; Forssén et al., 2006; Garnier et al., 2007; Voelkel and Strzemiecka, 2007; Ahmad and Guiochon, 2007). In order to solve the inverse problem of gas-liquid adsorption considering the two-layer isotherm given by Eq. (32), it was necessary to design two different experiments. One to estimate $K_2(T)$ and \hat{a} , called experiment 1, and another one to estimate λ , called experiment 2. In all cases studied the sensitivity to $K_1(T)$ is low and therefore this parameter was not estimated with the inverse problem solution.

In Fig. 10 are shown the sensitivity coefficients related to the parameters $K_1(T)$, $K_2(T)$, λ and \hat{a} in experiment 1. It is observed that the sensitivity to $K_2(T)$ and \hat{a} for BSA (Bovine Serum Albumin) are higher than the sensitivity to the other parameters and their shapes are different.

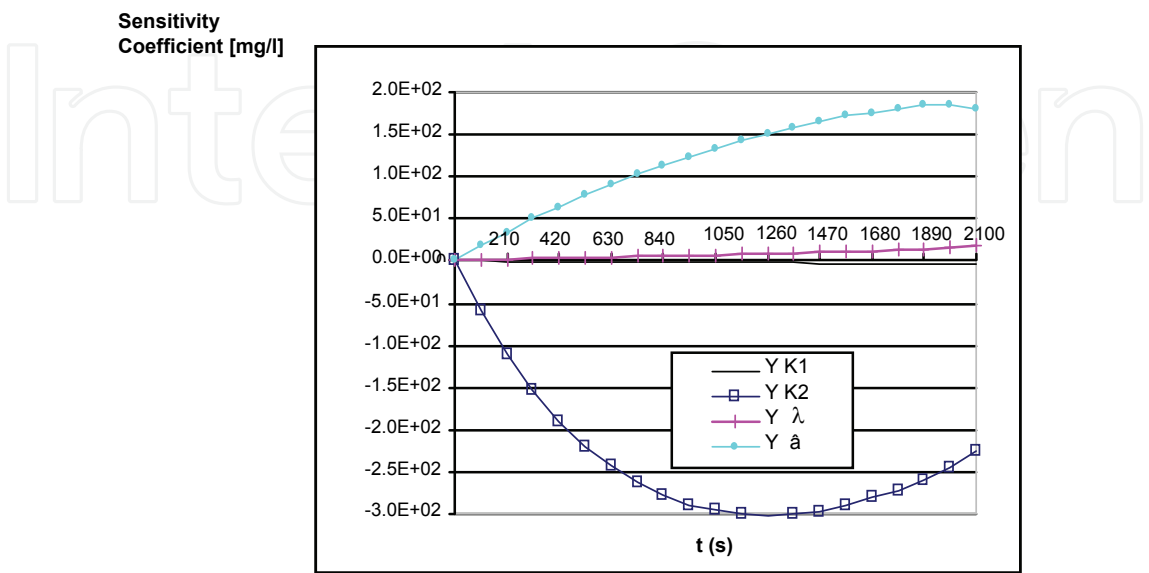


Fig. 10. Scaled sensitivity coefficients for BSA - Experiment 1.

In Fig. 11 are shown the sensitivity coefficients related to the parameters $K_1(T)$, $K_2(T)$, λ and \hat{a} for BSA in experiment 2. It is observed that the sensitivity to λ is higher than the sensitivity to the other parameters.

Another important tool used in the design of experiments is the study of the matrix $\mathbf{SC}^T\mathbf{SC}$, that is, maximizing the determinant of the matrix $\mathbf{SC}^T\mathbf{SC}$ results in higher sensitivity and uncorrelation (Dowding et al., 1999).

The difference between the two experiments is related to the BSA concentration, being larger in the first experiment (see Table 12).

In Fig. 12 are shown the values of the determinant of the matrix $\mathbf{SC}^T\mathbf{SC}$ for BSA in experiment 1. The designed experiment is marked with a full square. Its choice is justified by the small gain in sensitivity considering the operational difficulties in using a longer column or a higher superficial velocity.

Considering the analysis of the sensitivity graphs and the determinant of the matrix $\mathbf{SC}^T\mathbf{SC}$, two experiments were designed, one to estimate $K_2(T)$ and \hat{a} , and another to estimate λ , as shown in Table 12.

The results achieved using the ANN, LM 1 (gradient approximated by FDM), LM 2 (gradient approximated by ANN), SA and hybrid combinations, for different standard deviations for the measurements errors, σ , are shown in Tables 13 and 14.

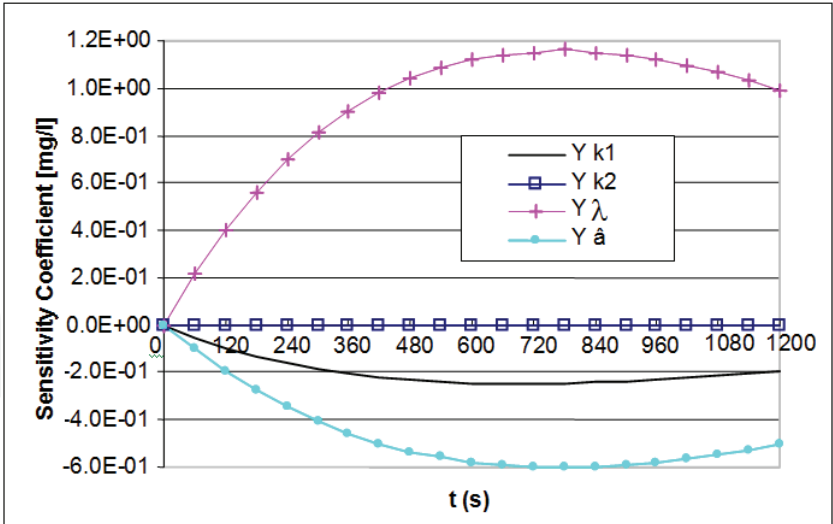


Fig. 11. Scaled sensitivity coefficients for BSA – Experiment 2.

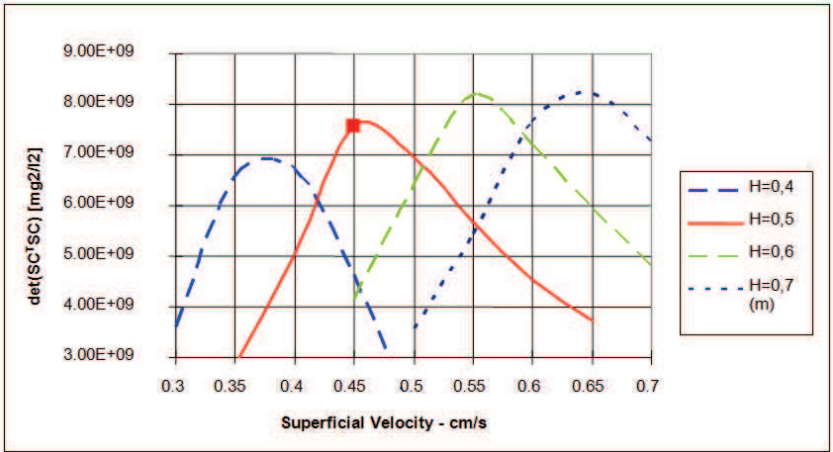


Fig. 12. Matrix $Y^T Y$ determinant for BSA – Experiment 1.

| | Units | Experiment | |
|--|------------------|----------------|-----------|
| | | 1 | 2 |
| Estimated parameters | - | K_2, \hat{a} | λ |
| Initial solute concentration, C_{b0} | g/m ³ | 1,000 | 10 |
| Bubble column height, H | m | 0.50 | 0.80 |
| Superficial velocity, v_g | m/s | 4.50E-3 | 1.00E-3 |
| First measurement | s | 210 | 120 |
| time measurement steps | s | 210 | 120 |
| Last measurement | s | 2100 | 1200 |

Table 12. Reference values for the designed experiment (Lugon 2005, Lugon et al., 2009).

In Table 13 are presented the results obtained for the estimation of $K_2(T)$ and \hat{a} , using the designed experiment number 1. Test cases 3-9 used simulated artificial data generated with the direct problem solution corrupted with white gaussian noise with standard deviation $\sigma = 10mg / l$, which corresponds to measurement errors of the order of 4%. While in test cases

numbers 1, 2, 3, 4 and 8 the initial guesses are $K_2 = 0,0080\text{ mg} / (m^2\text{ wt}\%)$ and $\hat{a} = 0,100\text{ m}^2 / \text{mg}$, in test cases numbers 6, 7 and 9 the initial guesses are the estimates obtained with the ANN.

| Case | Method | σ | Information | k_2 | \hat{a} | Time (s) | S [mg ² /l ²] Eq. (39a) |
|------|-----------------------------------|----------|-----------------------------|---------|-----------|----------|--|
| 1 | LM 1 (grad. FDM) | 0 | Result \vec{Z}_{LM}^{FDM} | 0.01040 | 0.322 | 169 | 0 |
| 2 | LM 2 (grad. ANN) | 0 | Result \vec{Z}_{LM}^{ANN} | 0.01040 | 0.322 | 80 | 0 |
| 3 | LM 1 (grad. FDM) | 10 | Result \vec{Z}_{LM}^{FDM} | 0.00790 | 0.158 | 170 | 8.39 |
| 4 | LM 2 (grad. ANN) | 10 | Result \vec{Z}_{LM}^{ANN} | 0.00805 | 0.157 | 78 | 8.64 |
| 5 | RNA | 10 | Result \vec{Z}_{ANN} | 0.01101 | 0.377 | 1 | 6.81 |
| 6 | LM 1 (grad. FDM) | 10 | Result \vec{Z}_{LM}^{FDM} | 0.01080 | 0.335 | 172 | 6.27 |
| 7 | LM 2 (grad. ANN) | 10 | Result \vec{Z}_{LM}^{ANN} | 0.01058 | 0.314 | 79 | 5.68 |
| 8 | SA (2.000 evaluations) | 10 | Result \vec{Z}_{SA} | 0.01050 | 0.312 | 6034 | 4.22 |
| 9 | ANN-LM-SA SA (200 evaluations) | 10 | Result \vec{Z}_{LM}^{ANN} | 0.01101 | 0.377 | 682 | 4.16 |
| | | | Result \vec{Z}_{LM}^{ANN} | 0.01058 | 0.335 | | |
| | | | Result \vec{Z}_{SA} | 0.01054 | 0.314 | | |

Table 13. Results obtained using ANN, LM 1, LM 2, SA and hybrid combinations for experiment 1.

In Table 14 are presented the results obtained for the estimation of λ , using the designed experiment number 2.

The exact values used are: $k_2 = 0.0104\text{mg} / (m^2\text{ wt}\%)$ and $\hat{a} = 0.322\text{ m}^2 / \text{mg}$.

| Case | Method | σ | Information | λ | Time (s) | S [mg ² /l ²] Eq. (39a) |
|------|-----------------------------------|----------|-----------------------------|-----------|----------|--|
| 1 | LM 1 (grad. FDM) | 0 | Result \vec{Z}_{LM}^{FDM} | 1.117 | 40 | 0 |
| 2 | LM 2 (grad. ANN) | 0 | Result \vec{Z}_{LM}^{ANN} | 1.117 | 29 | 0 |
| 3 | LM 1 (grad. FDM) | 0.1 | Result \vec{Z}_{LM}^{FDM} | 1.159 | 45 | 7.96 |
| 4 | LM 2 (grad. ANN) | 0.1 | Result \vec{Z}_{LM}^{ANN} | 1.159 | 30 | 7.96 |
| 5 | RNA | 0.1 | Result \vec{Z}_{ANN} | 1.432 | 1 | 202.9 |
| 6 | LM 1 (grad. FDM) | 0.1 | Result \vec{Z}_{LM}^{FDM} | 1.159 | 6 | 7.96 |
| 7 | LM 2 (grad. ANN) | 0.1 | Result \vec{Z}_{LM}^{ANN} | 1.159 | 4 | 7.96 |
| 8 | SA (2.000 evaluations) | 0.1 | Result \vec{Z}_{SA} | 1.099 | 5937 | 10.12 |
| 9 | ANN-LM-SA SA (200 evaluations) | 0.1 | Result \vec{Z}_{ANN} | 1.432 | 601 | 7.92 |
| | | | Result \vec{Z}_{LM}^{ANN} | 1.159 | | |
| | | | Result \vec{Z}_{SA} | 1.156 | | |

The exact value used is: $\lambda = 1.117\text{ m}^2 / \text{mg}$.

Table 14. Results obtained using ANN, LM 1, LM 2, SA and hybrid combinations for experiment 2.

Test cases 3-9 used simulated artificial data generated with the direct problem solution corrupted with white gaussian noise with standard deviation $\sigma = 0.10 \text{ mg/l}$, which corresponds to measurement errors of the order of 3%. While in test cases numbers 1, 2, 3, 4 and 8 the initial guess is $\lambda = 0.700 \text{ m}^2 / \text{mg}$, in test cases numbers 6, 7 and 9 the initial guesses are the estimates obtained with the ANN.

6. Conclusions

6.1 Radiative Transfer

6.1.1 Estimation of $\{\tau_0, \omega, \rho_1, \rho_2\}$ using LM-SA combination

A combination of SA (global optimization method) and LM (local optimization method) was used to solve the inverse radiative transfer problem. It was demonstrated its effectiveness in the solution of this type of problems since one can guarantee the convergence to a good approximation of the global optimum with higher accuracy and less computational effort if it is compared with the application of any global optimization method alone.

6.1.2 Estimation of $\{\omega, \tau_0, A_1, A_2\}$ using SA and DE

In the present work, the effectiveness of using Differential Evolution and Simulated Annealing for the estimation of radiative properties through an inverse problem approach was analyzed. In this sense, four benchmark cases were studied and it was possible to conclude that both algorithms led to good results for an acceptable number of generations. It should be pointed out that the Differential Evolution Algorithm led to optimal values that are very similar to those obtained by Simulated Annealing, requiring however a smaller number of objective function evaluations. This result was expected, since for the Simulated Annealing Algorithm, for a given iteration, every "temperature" is submitted to a proper number of internal iterations for refinement purposes making the evolutionary process longer, thus increasing the total processing time. On the other hand, as previously mentioned in the works of Storn and Price (1995), Storn (1999) and Angira and Babu (2005), the number of evaluations of the objective function resulting from the Differential Evolution Algorithm is smaller because the evolution scheme is much simpler.

Another interesting aspect is that by adding noise to the synthetic experimental points result an increase in the objective function values, as observed in Tables 6 to 9. Such a behavior was previously expected since noise does not permit the convergence of the optimization algorithm to the exact values of the parameters. Consequently, the user should be aware of this behavior when using real experimental data, which is always affected by noise.

6.2 Drying (Simultaneous Heat and Mass Transfer)

The direct problem of simultaneous heat and mass transfer in porous media modeled with Luikov equations can be solved using the finite difference method, yielding the temperature and moisture distribution in the media, when the geometry, the initial and boundary conditions, and the medium properties are known.

Inverse problem techniques can be useful to estimate the medium properties when they are not known. After the use of an experiment design technique, the hybrid combination ANN-LM-SA resulted in good estimates for the drying inverse problem using artificially generated data.

The design of experiments technique is of great importance for the success of the estimation efforts, while previous works studied the estimation of Lu , Pn , Ko , Bi_q and Bi_m , in this work it was considered Lu , δ , r/c , h/k and h_m/k_m . The main advantage of such approach is to be able to design an "optimum" experiment using different medium width, l , porous medium and air temperature difference, $T_s - T_0$, and porous medium and air moisture potential difference, $u_0 - u^*$.

The combination of deterministic (LM) and stochastic (ANN and SA) methods achieved good results, reducing the time needed and not being retained by local minima. The use of ANN to obtain the derivatives in the first steps of the LM method reduced the time required for the solution of the inverse problem.

6.3 Gas-liquid Adsorption

After the use of an experiment design technique, the hybrid combination ANN-LM-SA resulted in good solutions for the gas-liquid adsorption isotherm inverse problem.

The use of the ANN to obtain the derivatives in the first step of the LM method reduced the time necessary to solve the inverse problem.

7. References

- Ahmad, T. and Guiochon, G, 2007, Numerical determination of the adsorption isotherms of tryptophan at different temperatures and mobile phase composition, J. of Chromatography A, v. 1142, pp. 148-163.
- Alifanov, O. M., 1974, Solution of an Inverse Problem of Heat Conduction by Iteration Methods, J. of Engineering Physics, Vol.26, pp.471-476.
- Angira, R. and Babu, B. V., 2005, Non-dominated Sorting Differential Evolution (NSDE): An Extension of Differential Evolution for Multi-objective Optimization, In Proceedings of the 2nd Indian International Conference on Artificial Intelligence (IICAI-05).
- Artyukhin, E. A, 1982, Recovery of the Temperature Dependence of the Thermal Conductivity Coefficient from the Solution of the Inverse Problem, High Temperature, Vol.19, No.5, pp.698-702.
- Babu, B. V. and Angira, R., 2001, Optimization of Thermal Cracker Operation using Differential Evolution, in Proceedings of International Symposium and 54th Annual Session of IICChE (CHEMCON-2001).
- Babu, B. V. and Sastry, K. K. N., 1999, Estimation of Heat-transfer Parameters in a Trickle-bed Reactor using Differential Evolution and Orthogonal Collocation, Computers & Chemical Engineering, Vol. 23, pp. 327-339.
- Babu, B. V. and Singh, R. P., 2000, Synthesis and Optimization of Heat Integrated Distillation Systems Using Differential Evolution, in Proceedings of All-India seminar on Chemical Engineering Progress on Resource Development: A Vision 2010 and Beyond, IE (I).

- Babu, B. V. and Gaurav, C., 2000, Evolutionary Computation Strategy for Optimization of an Alkylation Reaction, in Proceedings of International Symposium and 53rd Annual Session of IChE (CHEMCON-2000).
- Baltes, M., Schneider, R., Sturm, C., and Reuss, M., 1994, Optimal Experimental Design for Parameter Estimation in Unstructured Growth Models, *Biotechnology Programming*, vol. 10, pp. 480-491.
- Becceneri, J. C., Stephany, S., Campos Velho, H. F. and Silva Neto, A. J., 2006, "Solution of the Inverse Problem of Radiative Properties Estimation with the Particle Swarm Optimization Technique", 14th Inverse Problems in Engineering Seminar, Ames, USA.
- Beck, J. V., Blackwell, B. and St. Clair Jr., C. R., 1985, *Inverse Heat Conduction*, Wiley, New York.
- Beck, J. V., 1988, Combined Parameter and Function Estimation in Heat Transfer with Application to Contact Conductance, *J. Heat Transfer*, v. 110, pp. 1046-1058.
- Borukhov, V. T. and Kolesnikov, P. M., 1988, Method of Inverse Dynamic Systems and Its Application for Recovering Internal Heat Sources, *Int. J. Heat Mass Transfer*, Vol.31, No.8, pp.1549-1556.
- Carita Montero, R. F., Roberty, N. C. and Silva Neto, A. J., 2000, Absorption Coefficient Estimation in Two-Dimensional Participating Media Using a Base Constructed with Divergent Beams, *Proc. 34th National Heat Transfer Conference*, Pittsburgh, USA.
- Carvalho, G. and Silva Neto, A. J., 1999, An Inverse Analysis for Polymers Thermal Properties Estimation, *Proc. 3rd International Conference on Inverse Problems in Engineering: Theory and practice*, Port Ludlow, USA.
- Cazzador, L. and Lubenova, V., 1995, Nonlinear Estimation of Specific Growth Rate for Aerobic Fermentation Processes, *Biotechnology and Bioengineering*, vol. 47, pp. 626-634.
- Chalhoub, E. S., Campos Velho, H. F., and Silva Neto, A. J., 2007a, A Comparison of the Onedimensional Radiative Transfer Problem Solutions obtained with the Monte Carlo Method and Three Variations of the Discrete Ordinates Method, *Proc. 19th International Congress of Mechanical Engineering - COBEM*.
- Chalhoub, E. S., Silva Neto, A. J. and Soeiro, F. J. C. P., 2007b, Estimation of Optical Thickness and Single Scattering Albedo with Artificial Neural Networks and a Monte Carlo Method, *Inverse Problems, Design and Optimization Symposium*, vol. 2, pp. 576-583, Miami.
- Chiou, J. P. and Wang, F. S., 1999, Hybrid Method of Evolutionary Algorithms for Static and Dynamic Optimization Problems with Application to a Fed-batch Fermentation Process, *Computers & Chemical Engineering*, vol. 23, pp. 1277-1291.
- Coelho L. S. and Mariani V. C., 2007, Improved Differential Evolution Algorithms for Handling Economic Dispatch Optimization with Generator Constraints, *Energy Conversion and Management*, 48, 2007, 1631-1639.
- Cuco, A. P. C., Silva Neto, A. J., Campos Velho, H. F. and de Sousa, F. L., 2009 Solution of an Inverse Adsorption Problem with an Epidemic Genetic Algorithm and the Generalized Extremal Optimization Algorithm, *Inverse Problems in Science and Engineering*. Vol. 17, No. 3, pp. 289-302
- Dantas, L. B., Orlande, H.R.B. and Cotta, R. M., 2003, An Inverse Problem of Parameter Estimation for Heat and Mass Transfer in Capillary Porous Media, *Int. J. Heat Mass Transfer*, v. 46, pp. 1587-1598.
- Deckwer, W. R. and Schumpe, A., 1993, Improved Tools for Bubble Columns Reactor Design and Scale-up, *Chem. Eng. Sc.*, v.48, No., pp. 889-911.

- Denisov, A. M. and Solo'Yera, S. I., 1993, The Problem of Determining the Coefficient in the Non-Linear Stationary Heat-Conduction Equation, *Comp. Math. Phys.*, Vol.33, No. 9, pp.1145-1153.
- Denisov, A. M., 2000, Inverse Problems of Absorption Dynamics, Minisymposium on Inverse Problems In Medicine, Engineering and Geophysics, XXIII Brazilian Congress on Applied and Computational Mathematics Invited Lecture, Santos Brasil.
- Dowding, K. J., Blackwell, B. F. and Cochran, R. J., 1999, Applications of Sensitivity Coefficients for Heat Conduction Problems, *Numerical Heat Transfer, Part B*, v. 36, pp. 33-55.
- Forssén, P., Arnell, R. and Fornstedt, T., 2006, An improved algorithm for solving inverse problems in liquid chromatography, *Computers and Chemical Engineering*, v.30, pp.1381-1391.
- Galski, R. L., de Sousa, F. L., Ramos, F. M. and Silva Neto, A. J., 2009. Application of a GEO+SA Hybrid Optimization Algorithm to the Solution of an Inverse Radiative Transfer Problem, *Inverse Problems in Science and Engineering*. Vol. 17, No. 3, pp. 321-334.
- Goldberg, D. E. 1989, "Genetic Algorithms in Search, Optimization, and Machine Learning", MA:Addison-Wesley.
- Garnier, C., Görner, T., Villiéras, F., De Donato, Ph., Polakovic, M., Bersillon, J. L. and Michot, L. J., 2007, Activated carbon surface heterogeneity seen by parallel probing by inverse liquid chromatography at the solid/liquid interface and by gas adsorption analysis at the solid/ gas interface, *Carbon*, v. 45, pp. 240-247.
- Graham, D. E. and Phillips, M. C., 1979, Proteins at Liquid Interfaces, II. Adsorption Isotherms, *J. Colloid and Interface Science*, v. 70, No. 3, pp. 415-426.
- Hanan, N. P., 2001, "Enhanced Two-layer Radiative Transfer Scheme for a Land Surface Model with a Discontinuous Upper Canopy". *Agricultural and Forest Meteorology*, vol. 109, pp. 265-281.
- Haut, B. and Cartage, T., 2005, Mathematical Modeling of Gas-liquid Mass Transfer Rate in Bubble Columns Operated in the Heterogeneous Regime, *Chem. Eng. Science*, v. 60, n. 22, pp. 5937-5944.
- Haykin, S., 1999, *Neural Networks - A Comprehensive Foundation*, Prentice Hall.
- Ho, C.-H. and Özisik, M. N., 1989, An Inverse Radiation Problem, *Int. J. Heat Mass Transfer*, Vol.32, No.2, pp.335-341.
- Huang, C. H. and Yeh, C. Y., 2002, An Inverse Problem in Simultaneous Estimating the Biot Number of Heat and Moisture Transfer for a Porous Material, *Int. J. Heat Mass Transfer*, v. 45, pp. 4643-4653.
- Kauati, A. T., Silva Neto, A. J. and Roberty, N. C., 1999, A Source-Detector Methodology for the Construction and Solution of the One-Dimensional Inverse Transport Equation, *Proc. 3rd International Conference on Inverse Problems in Engineering: Theory and Practice*, Port Ludlow, USA.
- Kirkpatrick, S., Gellat, Jr., C. D. and Vecchi, M. P., 1983 Optimization by Simulated Annealing, *Science*, v. 220, pp. 671-680.
- Knupp, D. C., Silva Neto, A. J. and Sacco, W. F., 2007, Estimation of Radiative Properties with the Particle Collision Algorithm, *Inverse Problems, Design and Optimization Symposium*, Miami, Florida, USA, April, 16-18.
- Krishna, R. and van Baten, J. M., 2003, Mass Transfer in Bubble Columns, *Catalysis Today*, v. 79-80, pp. 67-75.

- Lobato, F. S. and Steffen Jr., V., 2007, Engineering System Design with Multi-Objective Differential Evolution, In Proceedings in 19th International Congress of Mechanical Engineering - COBEM.
- Lobato, F. S., Steffen Jr., V., Arruda, E. B. and Barrozo, M. A. S., 2008, Estimation of Drying Parameters in Rotary Dryers using Differential Evolution, Journal of Physics: Conference Series, Vol. 135, doi:10.1088/1742-6596/135/1/012063.
- Lobato, F. S., Steffen Jr. V. and Silva Neto, A. J., 2009, Solution of Inverse Radiative Transfer Problems in Two-Layer Participating Media with Differential Evolution, Inverse Problems in Science and Engineering, Vol.115, p. 1054-1064, 2009, doi: 10.1080/17415970903062054.
- Lobato, F. S., Steffen Jr., V. and Silva Neto, A. J., 2010, A Comparative Study of the Application of Differential Evolution and Simulated Annealing in Inverse Radiative Transfer Problems, Journal of the Brazilian Society of Mechanical Sciences and Engineering, Accepted for publication.
- Lugon Jr., J. and Silva Neto, A. J., 2004, Deterministic, Stochastic and Hybrid Solutions for Inverse Problems in Simultaneous Heat and Mass Transfer in Porous Media, Proc. 13th Inverse Problems in Engineering Seminar, pp. 99-106, Cincinnati, USA.
- Lugon Jr., J., 2005, Gas-liquid Interface Adsorption and One-dimensional Porous Media Drying Inverse Problems Solution, D.Sc Thesis, Universidade do Estado do Rio de Janeiro (in Portuguese).
- Lugon Jr., J, Silva Neto, A. J. and Santana, C. C., 2009, A Hybrid Approach with Artificial Neural Networks, Levenberg-Marquardt and Simulated Annealing Methods for the Solution of Gas-Liquid Adsorption Inverse Problems, Inverse Problems in Science and Engineering, Vol. 17, No. 1, pp.85-96.
- Lugon Jr., J and Silva Neto, A. J., 2010, Solution of Porous Media Inverse Drying Problems Using a Combination of Stochastic and Deterministic Methods, Journal of the Brazilian Society of Mechanical Sciences and Engineering, Accepted for publication.
- Luikov, A. V. and Mikhailov, Y. A., 1965, Theory of Energy and Mass Transfer, Pergamon Press, Oxford, England.
- Maciejewski L., Myszkowski W. and Zietek G., 2007, Application of Differential Evolution Algorithm for Identification of Experimental Data, The Archive of Mechanical Engineering, 4, 327-337.
- Mariani V. C., Lima A. G. B. and Coelho L. S., 2008, Apparent Thermal Diffusivity Estimation of the Banana during Drying using Inverse Method, Journal of Food Engineering, 85, 569-579.
- Marquardt, D. W., 1963, An Algorithm for Least-Squares Estimation of Nonlinear Parameters, J. Soc. Industr. Appl. Math., v. 11, pp. 431-441.
- McCormick, N. J., 1986, Methods for Solving Inverse Problems for Radiation Transport-an Update, Transp. Theory Statist. Phys., Vol.15, pp.759-772.
- McCormick, N. J., 1992, Inverse Radiative Transfer Problems: A Review, Nuclear Science and Engineering, Vol.112, pp.185-198.
- McCormick, N. J., 1993, Inverse Photon Transport Methods for Biomedical Applications, Proc. 1st International Conference on Inverse Problems in Engineering: Theory and Practice, Florida, USA., pp.253-258.
- Metropolis, N., Rosenbluth, A. W., Teller, A. H. and Teller, E., 1953, Equation of State Calculations by Fast Computing Machines, J. Chem. Physics, v.21, pp.1087-1092.

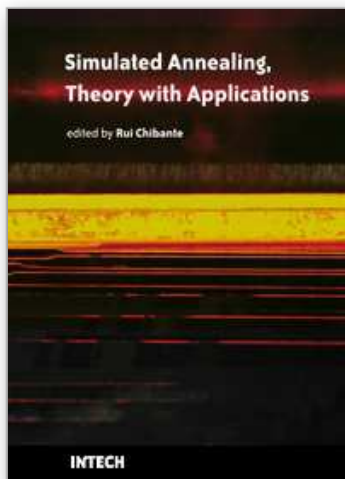
- Mikhailov, M. D. and Özisik, M. N., 1994, *Unified Analysis and Solutions of Heat and Mass Diffusion*, Dover Publications, Inc.
- Mouza, A. A., Dalakoglou, G. K. and Paras, S. V., 2005, Effect of Liquid Properties on the Performance of Bubble Column Reactors with Fine Pore Spargers, *Chem. Eng. Science*, v. 60, n. 5, pp. 1465-1475.
- Moura Neto, F. D. and Silva Neto, A. J., 2000, Two Equivalent Approaches to Obtain the Gradient in Algorithms for Function Estimation in Heat Conduction Problems, *Proc. 34th National Heat Transfer Conference*, Pittsburgh, USA.
- Muniz, W. B., Campos Velho, H. F. and Ramos, F. M., 1999, A Comparison of Some Inverse Methods for Estimating the Initial Condition of the Heat Equation, *Journal of Computational and Applied Mathematics*, Vol.103, pp.145-163.
- Mwithiga, G., and Olwal, J. O., 2005, The drying kinetics of kale (*Brassica oleracea*) in a convective hot air dryer, *J. of Food Engineering*, v. 71, No. 4, pp. 373-378.
- Orlande, H. R. B. and Özisik, M. N., 1993, Determination of the Reaction Function in a Reaction-Diffusion Parabolic Problem, *Proc. 1st International Conference on Inverse Problems in Engineering: Theory and Practice*, Florida, USA, pp.117-124.
- Özisik, M. N., 1973, *Radiation Transfer and Iterations with Conduction and Convection*, John Wiley.
- Özturk, S. S., Schumpe, A. and Deckwer, W.D., 1987, Organic Liquids in a Bubble Column: Holdups and Mass Transfer Coefficients, *AIChE Journal*, v. 33, No. 9, pp. 1473-1480.
- Santana, C. C. and Carbonell, R. G., 1993a, Waste Minimization by Flotation: Recovery of Proteins and Other Surface-Active Compounds, *3rd Int. Conf. Waste Management*, Bahia, Brazil.
- Santana, C. C. and Carbonell, R. G., 1993b, Adsorptive Bubble Separation as a Means of Reducing Surface-Active Contaminants in Industrial Wastewaters, *Proc. Int. Symp. on Heat and Mass Transfer*, Cancun, Mexico, pp. 1-11.
- Santana, C. C., 1994, Adsorptive Bubble Separation Process as a Means of Reducing Surface-Active Contaminants in Industrial Wastewaters, *Brazilian J. Engineering- Chemistry*, v. 5.
- Silva Neto, A. J. and Özisik, M. N., 1993a, Inverse Problem of Simultaneously Estimating the Timewise-varying Strength of Two Plane Heat Sources, *J. Applied Physics*, Vol. 73, no 5, pp. 2132-2137.
- Silva Neto, A. J. and Özisik, M. N., 1993b, Simultaneous Estimation of Location and Timewise-varying Strength of a Plane Heat Source, *Numerical Heat Transfer*, Vol. 24, pp. 467-477.
- Silva Neto, A. J. and Özisik, M. N., 1994, The Estimation of Space and Time Dependent Strength of a Volumetric Heat Source in a One-Dimensional Plate, *Int. J. Heat Mass Transfer*, Vol. 37, no 6, pp. 909-915.
- Silva Neto, A. J. and Özisik, M. N., 1995, An Inverse Problem of Simultaneous Estimation of Radiation Phase Function, Albedo and Optical Thickness, *J. Quant. Spectrosc. Radiat. Transfer*, Vol.53, No.4, pp.397-409.
- Silva Neto, A. J. and Moura Neto, F. D., 2005, *Inverse Problems: Fundamental Concepts and Applications*, EdUERJ, Rio de Janeiro. (in Portuguese).
- Silva Neto, A. J. and Soeiro, F. J. C. P., 2003, Solution of Implicitly Formulated Inverse Heat Transfer Problems with Hybrid Methods, *Mini-Symposium Inverse Problems from Thermal/Fluids and Solid Mechanics Applications - 2nd MIT Conference on Computational Fluid and Solid Mechanics*, Cambridge, USA.

- Silva Neto, A. J. and Soeiro, F. J. C. P., 2002, "Estimation of the Phase Function of Anisotropic Scattering with a Combination of Gradient Based and Stochastic Global Optimization Methods. In Proceedings of 5th World Congress on Computational Mechanics, Vienna, Austria, July, 7-12.
- Silva Neto, C. A. and Silva Neto, A. J., 2003, Estimation of Optical Thickness, Single Scattering Albedo and Diffuse Reflectivities with a Minimization Algorithm Based on an Interior Points Method. In Proceedings of 17th International Congress of Mechanical Engineering, ABCM, São Paulo, Brazil.
- Silva Neto, A. J. and Soeiro, F. J. C. P., 2006, The Solution of an Inverse Radiative Transfer Problem with the Simulated Annealing and Levenberg-Marquardt Methods, *Boletim da SBMAC*, Vol. VII, No. 1, pp. 17-30.
- Soeiro, F. J. C. P., Carvalho, G. and Silva Neto, A. J., 2000, Thermal Properties Estimation of Polymeric Materials with the Simulated Annealing Method, *Proc. 8th Brazilian Congress of Engineering and Thermal Sciences*, Porto Alegre, Brazil (in Portuguese).
- Soeiro, F.J.C.P., Soares, P.O. and Silva Neto, A.J., 2004, Solution of Inverse Radiative Transfer Problems with Artificial Neural Networks and Hybrid Methods, *Proc. 13th Inverse Problems in Engineering Seminar*, pp. 163-169, Cincinnati, USA.
- Souza, F. L., Soeiro, F. J. C. P., Silva Neto, A. J., and Ramos, F. M., 2007, Application of the Generalized External Optimization Algorithm to an Inverse Radiative Transfer Problem, *Inverse Problems in Science and Engineering*, 15, 7, 699-714.
- Souto, R. P., Stephany, S., Becceneri, J. C., Campos Velho, H. F. and Silva Neto, A. J., 2005, Reconstruction of Spatial Dependent Scattering Albedo in a Radiative Transfer Problem using a Hybrid Ant Colony System Implementation Scheme, *6th World Congress on Structural and Multidisciplinary Optimization*, Rio de Janeiro, Brazil.
- Storn, R., 1995, "Differential Evolution Design of an IIR-Filter with Requirements for Magnitude and Group Delay," *International Computer Science Institute*, TR-95-026.
- Storn, R., 1999, System Design by Constraint Adaptation and Differential Evolution, *IEEE Transactions on Evolutionary Computation*, vol. 3, pp. 22-34.
- Storn, R. and Price, K., 1995, Differential Evolution: A Simple and Efficient Adaptive Scheme for Global Optimization over Continuous Spaces, *International Computer Science Institute*, vol. 12, pp. 1-16.
- Storn, R., Price, K. and Lampinen, J. A., 2005, *Differential Evolution - A Practical Approach to Global Optimization*, Springer - Natural Computing Series.
- Su, J. and Silva Neto, A. J., 2001, Two-dimensional Inverse Heat Conduction Problem of Source Strength Estimation in Cylindrical Rods. *Applied Mathematical Modelling*, Vol. 25, pp. 861-872.
- Su, J., Silva Neto, A. J. and Lopes, A. B., 2000, Estimation of Unknown Wall Heat Flux in Turbulent Circular Pipe Flow, *Proc. 8th Brazilian Congress of Engineering and Thermal Sciences*, Porto Alegre, Brazil (in Portuguese).
- Sundman, L. K., Sanchez, R. and McCormick, N. J., 1998, Ocean Optical Source Estimation with Widely Spaced Irradiance Measurements, *Applied Optics*, Vol.37, No.18, pp.3793-3803.
- Voelkel, A. and Strzemieska, B., 2007, Characterization of fillers used in abrasive articles by means of inverse gas chromatography and principal components analysis, *Int. J. of Adhesion and Adhesives*, v. 27, pp. 188-194.

- Wang, F. S., Su, T. L. and Jang, H. J., 2001, Hybrid Differential Evolution for Problems of Kinetic Parameter Estimation and Dynamic Optimization of an Ethanol Fermentation Process, *Industry Engineering Chemical Research*, vol. 40, pp. 2876-2885.
- Wang, J.-Z., Su, J. and Silva Neto, A. J., 2000, Source Term Estimation in Non-Linear Heat Conduction Problems with Alifanov's Iterative Regularization Method, *Proc. 8th Brazilian Congress of Engineering and Thermal Sciences*, Porto Alegre, Brazil (in Portuguese).
- Yan, L., Fu, C. L. and Yang, F. L., 2008, The Method of Fundamental Solutions for the Inverse Heat Source Problem, *Engineering Analysis with Boundary Elements*, Vol. 32, pp. 216-222.
- Yang, F. L., Yan, L. and Wei, T., 2009, Reconstruction of Part of a Boundary for the Laplace Equation by using a Regularized Method of Fundamental Solutions, *Inverse Problems in Science and Engineering*, vol. 17, pp. 1113-1128.

Acknowledgements

The authors acknowledge the financial support provided by CNPq, Conselho Nacional de Desenvolvimento Científico e Tecnológico, FAPERJ, Fundação Carlos Chagas Filho de Amparo à Pesquisa do Estado do Rio de Janeiro, FAPESP, Fundação de Amparo à Pesquisa do Estado de São Paulo, and FAPEMIG, Fundação de Amparo à Pesquisa do Estado de Minas Gerais.



Simulated Annealing, Theory with Applications

Edited by Rui Chibante

ISBN 978-953-307-134-3

Hard cover, 292 pages

Publisher Sciyo

Published online 18, August, 2010

Published in print edition August, 2010

The book contains 15 chapters presenting recent contributions of top researchers working with Simulated Annealing (SA). Although it represents a small sample of the research activity on SA, the book will certainly serve as a valuable tool for researchers interested in getting involved in this multidisciplinary field. In fact, one of the salient features is that the book is highly multidisciplinary in terms of application areas since it assembles experts from the fields of Biology, Telecommunications, Geology, Electronics and Medicine.

How to reference

In order to correctly reference this scholarly work, feel free to copy and paste the following:

Antônio Silva Neto, Jader Lugon Junior, Francisco J. C. P. Soeiro, Luiz Biondi Neto, Cesar Costapinto Santana, Fran Sergio Lobato and Valder, Junior Steffen (2010). Application of Simulated Annealing and Hybrid Methods in the Solution of Inverse Heat and Mass Transfer Problems, Simulated Annealing, Theory with Applications, Rui Chibante (Ed.), ISBN: 978-953-307-134-3, InTech, Available from:
<http://www.intechopen.com/books/simulated-annealing--theory-with-applications/application-of-simulated-annealing-and-hybrid-methods-in-the-solution-of-inverse-heat-and-mass-trans>

INTECH
open science | open minds

InTech Europe

University Campus STeP Ri
Slavka Krautzeka 83/A
51000 Rijeka, Croatia
Phone: +385 (51) 770 447
Fax: +385 (51) 686 166
www.intechopen.com

InTech China

Unit 405, Office Block, Hotel Equatorial Shanghai
No.65, Yan An Road (West), Shanghai, 200040, China
中国上海市延安西路65号上海国际贵都大饭店办公楼405单元
Phone: +86-21-62489820
Fax: +86-21-62489821

© 2010 The Author(s). Licensee IntechOpen. This chapter is distributed under the terms of the [Creative Commons Attribution-NonCommercial-ShareAlike-3.0 License](https://creativecommons.org/licenses/by-nc-sa/3.0/), which permits use, distribution and reproduction for non-commercial purposes, provided the original is properly cited and derivative works building on this content are distributed under the same license.

IntechOpen

IntechOpen